



UNIVERSIDADE FEDERAL DO CEARÁ
CENTRO DE TECNOLOGIA
DEPARTAMENTO DE ENGENHARIA QUÍMICA
PROGRAMA DE PÓS-GRADUAÇÃO EM ENGENHARIA QUÍMICA

MATHEUS DE OLIVEIRA BARROS

**EFEITO DA MOAGEM DO AMIDO DE MILHO NA GELATINIZAÇÃO E NA
ESTABILIZAÇÃO COOPERATIVA DE EMULSÕES PICKERING COM QUITINA**

FORTALEZA

2025

MATHEUS DE OLIVEIRA BARROS

EFEITO DA MOAGEM DO AMIDO DE MILHO NA GELATINIZAÇÃO E NA
ESTABILIZAÇÃO COOPERATIVA DE EMULSÕES PICKERING COM QUITINA

Tese apresentada ao Programa de Pós-Graduação em Engenharia Química da Universidade Federal do Ceará, como requisito parcial à obtenção do título de Doutor em Engenharia Química. Área de concentração: Processos Químicos e Bioquímicos.

Orientadora: Dra. Morsyleide de Freitas Rosa.
Coorientador: Dr. Edy Sousa de Brito.

FORTALEZA

2025

MATHEUS DE OLIVEIRA BARROS

EFEITO DA MOAGEM DO AMIDO DE MILHO NA GELATINIZAÇÃO E NA
ESTABILIZAÇÃO COOPERATIVA DE EMULSÕES PICKERING COM QUITINA

Tese apresentada ao Programa de Pós-Graduação em Engenharia Química da Universidade Federal do Ceará, como requisito parcial à obtenção do título de Doutor em Engenharia Química. Área de concentração: Processos Químicos e Bioquímicos.

Aprovado em: 08/05/2025.

BANCA EXAMINADORA

Dra. Morsyleide de Feitas Rosa (Orientadora)
Universidade Federal do Ceará (UFC)

Dra. Fabia Karine Andrade
Universidade Federal do Ceará (UFC)

Dr. Rodrigo Silveira Vieira
Universidade Federal do Ceará (UFC)

Dr. Adriano Lincoln Albuquerque Mattos
Embrapa Agroindústria Tropical

Aos meus pais, Elidênia e Giano.

AGRADECIMENTOS

O presente trabalho foi realizado com apoio da Coordenação de Aperfeiçoamento de Pessoal de Nível Superior – Brasil (CAPES) – Código de Financiamento 001.

A conclusão deste trabalho não teria sido possível sem o apoio, a orientação e o incentivo de muitas pessoas e instituições, às quais expresso minha profunda gratidão.

Aos meus pais, Elidênia e Giano, e à minha família, minha base e meu porto seguro, agradeço por todo amor, apoio incondicional e incentivo ao longo de toda a minha trajetória. Cada gesto de carinho, cada palavra de encorajamento e cada sacrifício feito por mim foram fundamentais para que eu pudesse chegar até aqui. Esta conquista é, também, de vocês.

Ao Simba, meu cachorro, pelo apoio emocional e suporte nas noites de ansiedade e aperreio estudando e resolvendo pepinos do doutorado.

À minha orientadora Morsyleide agradeço a confiança, dedicação, paciência e pelos ensinamentos compartilhados ao longo desta jornada. Sua orientação foi essencial para o desenvolvimento deste trabalho e para meu crescimento acadêmico e pessoal.

Ao Dr. Edy Brito, meu coorientador, agradeço pela parceria, pelas contribuições valiosas e pelo incentivo à superação de desafios científicos.

Ao Programa de Pós-Graduação em Engenharia Química.

Agradeço às agências de fomento CAPES e CNPq, pelo apoio financeiro fundamental ao longo do meu percurso de formação.

À banca de qualificação, composta pelo Dr. Adriano Mattos e Dra. Ana Iraidy, agradeço pelas críticas construtivas, sugestões e contribuições que enriqueceram significativamente este trabalho.

Ao Bioproducts Institute, da University of British Columbia (UBC), e ao Professor Orlando Rojas, sou profundamente grato pela oportunidade de aprendizado e colaboração internacional. A experiência no Canadá foi transformadora tanto do ponto de vista científico quanto pessoal.

Aos funcionários e colegas do Laboratório de Tecnologia de Biomassa (LTB, Adriano, Men de Sá, Cléa, Alex, e aos queridos amigos Maíra, Jessica, Camila, Priscilla, Daniel, Carmélia, Renata, Sarah, Darlyson e Grazielly, deixo meu sincero agradecimento pelo apoio no dia a dia do laboratório, pela amizade e pelos momentos compartilhados, que tornaram esta trajetória mais leve e significativa.

A todas as pessoas que, direta ou indiretamente, contribuíram para a realização deste trabalho, meu muito obrigado.

RESUMO

Emulsões Pickering, ao contrário das convencionais estabilizadas por surfactantes, utilizam partículas coloidais como estabilizadores, eliminando a necessidade desses agentes que podem ser danosos à saúde e ao meio-ambiente. O nanoamido, obtido por moagem, representa uma abordagem sustentável em comparação à hidrólise ácida tradicional e pode ainda alterar propriedades do amido de forma interessante, como a sua temperatura de gelatinização. Para melhorar a estabilidade dessas partículas em emulsões, a funcionalização das cadeias do amido por oxidação com anidrido 2-octen-1-ilsuccínico (OSA) é usualmente empregada; porém, alternativas sustentáveis como micronização, plasma e combinação com outros polímeros naturais apresentam vantagens. A quitina, presente em fungos e exoesqueletos de artrópodes, destaca-se como estabilizador de emulsões Pickering devido a suas propriedades biocompatíveis e anti-inflamatórias, que são bastante atraentes para aplicações alimentícias. Este projeto busca explorar a eficácia da moagem de bolas na produção de partículas de amido de menor tamanho e verificar a modificação em suas propriedades. Posteriormente usar essas partículas coloidais obtidas em moinho de bolas juntamente com os nanocristais de quitina como técnica de combinação de polímeros para estabilização de emulsões Pickering. A moagem de bolas do amido se mostrou efetiva na redução de tamanho e foi capaz de diminuir a temperatura de gelatinização do amido, com tempos superiores a 10 h utilizando uma relação mássica de amidos para bolas de 1:20. A combinação do amido moído por 20 h com os nanocristais de quitina se mostrou eficiente na estabilização de emulsões Pickering quando utilizadas em concentrações iguais, produzindo uma emulsão com baixo tamanho de gotas (2.29 μm) e estabilidade à cremação superior a um mês de armazenamento em temperatura ambiente.

Palavras-chave: Amido; Emulsões Pickering; Quitina; Moagem; Mecanoquímica.

ABSTRACT

Pickering emulsions, unlike conventional ones stabilized by surfactants, use colloidal particles as stabilizers, eliminating the need for these agents that can be harmful to health and the environment. Nano-starch, obtained through milling, represents a sustainable approach compared to traditional acid hydrolysis and can also alter interesting properties of starch, such as its gelatinization temperature. To improve the stability of these particles in emulsions, functionalization of starch chains by oxidation with 2-octen-1-ylsuccinic anhydride (OSA) is usually employed; however, sustainable alternatives such as micronization, plasma, and combination with other natural polymers present advantages. Chitin, found in fungi and arthropod exoskeletons, stands out as a stabilizer for Pickering emulsions due to its biocompatible and anti-inflammatory properties, which are highly attractive for food applications. This project aims to explore the effectiveness of ball milling in producing smaller starch particles and verify the modification in their properties. Subsequently, using these colloidal particles obtained in a ball mill along with chitin nanocrystals as a polymer combination technique for stabilizing Pickering emulsions. Ball milling of starch has proven effective in size reduction and was able to decrease the starch gelatinization temperature, with milling times exceeding 10 hours using a starch-to-balls mass ratio of 1:20. The combination of starch milled for 20 hours with chitin nanocrystals proved efficient in stabilizing Pickering emulsions when used in equal concentrations, producing an emulsion with a low droplet size (2.29 μm) and creaming stability superior to one month of storage at room temperature.

Keywords: Starch; Pickering Emulsions; Chitin; Milling; Mechanochemistry.

LISTA DE FIGURAS

| | |
|---|----|
| Figure 1 – Schematic representation of a droplet in a Pickering emulsion (A) and a traditional emulsion (B) | 20 |
| Figure 2 – Chemical structures of amylose and amylopectin..... | 22 |
| Figure 3 – Scanning electron micrographs of starch, both control and milled samples. Scale bars: 20 μ m. | 34 |
| Figure 4 – Polarized light microscope images of starch. (a-b) control; (c-n) milled starch: (c-d) 10 h (milling time), 1:6 (mass ratio of starch to balls); (e-f) 20 h, 1:6; (g-h) 30 h, 1:6; (i-j) 10 h, 1:20; (k-l) 20 h, 1:20; (m-n) 30 h, 1:20. The darker images for each pair were taken under polarized light, and the lighter images were not. | 35 |
| Figure 5 – Infrared spectra in the 900 to 1110 cm^{-1} region for the samples of starch milled for 30 h (both ratios) and control starch. | 36 |
| Figure 6 – Amylose content (%) for all the starch samples, milled and control. | 37 |
| Figure 7 – TG (a) and DTG (b) curves for control and milled starch. | 38 |
| Figure 8 – Differential scanning calorimetry curves for control and milled starch. | 39 |
| Figure 9 – Diffractograms of the 1:6 (a) and 1:20 ratio (b) milled starch samples and the control sample..... | 40 |
| Figure 10 – Swelling power (a) and Solubility (b) of the native corn starch sample (Control) and the ball-milled starch samples. | 41 |
| Figure 11 – Films formed by oven drying starch suspensions (10%) at room temperature (30 $^{\circ}\text{C}$) using control and milled starches. | 44 |
| Figure 12 – Transmission electron microscopy (TEM) images of the starch nanoparticles (A) and chitin nanocrystals (B) under 30000x magnification. | 52 |
| Figure 13 – Microscopy of the different SNP:ChNC ratio emulsions, both control and HT, taken at day 0 with 4000x magnification..... | 53 |
| Figure 14 – Confocal Laser Scanning Microscopy (CLSM) images of the 1:1 HT sample, a couple hours after preparation. (A) Bright field image of the emulsion. (B) SNP particles stained with Nile Blue. (C) Sunflower oil droplets stained red. (D) ChNC stained with FITC..... | 54 |
| Figure 15 – Droplet size based on area of droplets for the different SNP:ChNC ratio emulsions for 150 days storage at 21 $^{\circ}\text{C}$, for control (A) and HT (B) samples. | 55 |

| | |
|--|----|
| Figure 16 – Zeta potential measurements of the aqueous phases (A) and the different SNP:ChNC ratio emulsions (B), for control and HT samples. | 56 |
| Figure 17 – Visual appearance of the control emulsions (non-heat-treated) and the heat-treated (HT) emulsions over time (150 days) with different ratios of SNP:ChNC. | 58 |
| Figure 18 – Creaming indexes of the heat treated emulsions control (A) and the HT emulsions (B) with different ratios of SNP:ChNC..... | 59 |
| Figure 19 – Instability index (A) and creaming velocity (B) obtained via accelerated stability analysis for the different SNP:ChNC ratio emulsions, both control and HT at 21 °C. | 60 |
| Figure 20 – Sedimentation velocity obtained via accelerated stability analysis for the different SNP:ChNC ratio aqueous phase, both control and HT..... | 61 |
| Figure 21 – Apparent viscosity (100s-1) for the different SNP:ChNC ratio emulsions (A) and their respective aqueous phase (B), both control and HT samples. | 62 |
| Figure 22 – Separation indexes for the studied HT Pickering emulsions under different temperatures (A) and pH (B) conditions, after 7 days of storage. | 63 |

LISTA DE TABELAS

| | |
|--|----|
| Table 1 – 995/1044 cm ⁻¹ band ratio for control and milled starch. | 35 |
| Table 2 – Gelatinization enthalpy, peak and end temperature of starch samples..... | 39 |
| Table 3 – Crystalline indexes (CrI) of the control and milled starch samples. | 40 |
| Table 4 – Rheological parameters of the control and milled starch samples. | 43 |

SUMÁRIO

| | | |
|---------------|--|-----------|
| 1 | INTRODUÇÃO GERAL | 14 |
| 2 | OBJETIVOS | 18 |
| 2.1 | Objetivo Geral | 18 |
| 2.1 | Objetivos Específicos..... | 18 |
| 3 | LITERATURE REVIEW | 19 |
| 3.1 | Problem Statement and Context | 19 |
| 3.2 | Pickering Emulsions | 20 |
| 3.3 | Starch Nanoparticles | 22 |
| 3.4 | Chitin Nanocrystals | 24 |
| 3.5 | Pickering applications in Food Systems | 25 |
| 4 | EFFECT OF BALL-MILLING ON STARCH CRYSTALLINE STRUCTURE, GELATINIZATION TEMPERATURE, AND RHEOLOGICAL PROPERTIES: TOWARDS ENHANCED UTILIZATION IN THERMOSENSITIVE SYSTEMS | 27 |
| 4.1 | Introduction | 27 |
| 4.2 | Materials and Methods | 29 |
| 4.2.1 | <i>Corn starch</i> | 29 |
| 4.2.2 | <i>Starch ball milling.....</i> | 29 |
| 4.2.3 | <i>Microscopy analysis.....</i> | 29 |
| 4.2.4 | <i>Fourier transform infrared spectroscopy (FTIR)</i> | 30 |
| 4.2.5 | <i>Amylose content.....</i> | 30 |
| 4.2.6 | <i>Thermogravimetric analysis (TGA)</i> | 30 |
| 4.2.7 | <i>Differential scanning calorimetry (DSC)</i> | 31 |
| 4.2.8 | <i>X-ray diffraction (XRD)</i> | 31 |
| 4.2.9 | <i>Swelling power (SP) and Solubility (S%)</i> | 31 |
| 4.2.10 | <i>Rheology.....</i> | 32 |

| | | |
|--------|--|----|
| 4.2.11 | <i>Film forming ability</i> | 32 |
| 4.2.12 | <i>ANOVA Analysis</i> | 33 |
| 4.3 | Results and discussion | 33 |
| 4.3.1 | <i>Microscopic analysis</i> | 33 |
| 4.3.2. | <i>Fourier transform infrared spectroscopy (FTIR)</i> | 35 |
| 4.3.3 | <i>Amylose content</i> | 37 |
| 4.3.4 | <i>Thermogravimetric analysis (TGA)</i> | 37 |
| 4.3.5 | <i>Differential scanning calorimetry (DSC)</i> | 38 |
| 4.3.6 | <i>X-ray diffraction (XRD)</i> | 40 |
| 4.3.7 | <i>Swelling power (SP) and Solubility (S%)</i> | 41 |
| 4.3.8 | <i>Rheology</i> | 42 |
| 4.3.9 | <i>Film forming ability</i> | 43 |
| 4.4 | Conclusions | 44 |
| 5 | OPTIMIZING PICKERING EMULSION STABILITY: UNVEILING THE SYNERGISTIC POTENTIAL OF STARCH NANOPARTICLES AND CHITIN NANOCRYSTALS. | 46 |
| 5.1 | Introduction | 46 |
| 5.2 | Materials and Method | 48 |
| 5.2.1 | <i>Materials</i> | 48 |
| 5.2.2 | <i>Preparation of the Pickering emulsions</i> | 49 |
| 5.2.3 | <i>Kinetic stability of emulsions</i> | 50 |
| 5.2.4 | <i>Emulsion morphology</i> | 50 |
| 5.2.5 | <i>Droplet size and Electrostatic charges</i> | 50 |
| 5.2.6 | <i>Stability analysis (pH and temperature)</i> | 51 |
| 5.2.7 | <i>Rheological properties</i> | 51 |
| 5.3 | Results and Discussion | 52 |
| 5.3.1 | <i>SNP and ChNC morphology and size</i> | 52 |

| | | |
|-------|--|----|
| 5.3.2 | <i>Emulsion droplet morphology</i> | 53 |
| 5.3.3 | <i>Droplet size measurements</i> | 55 |
| 5.3.4 | <i>Zeta potential</i> | 56 |
| 5.3.5 | <i>Long-term stability of the Pickering emulsions</i> | 57 |
| 5.3.6 | <i>Instability index, creaming velocity, and sedimentation</i> | 60 |
| 5.3.7 | <i>Viscosity assays</i> | 62 |
| 5.3.8 | <i>pH and temperature stability</i> | 63 |
| 5.4 | Conclusions | 64 |
| 5 | CONCLUSÕES GERAIS | 65 |
| | REFERÊNCIAS | 66 |

1 INTRODUÇÃO GERAL

Emulsões são formadas por uma fase dispersa em outra fase contínua. Geralmente, as substâncias que compõem essas fases não se misturam; desse modo moléculas de emulsificantes, que possuem extremidades com afinidade em ambas as fases, são necessárias para promover a estabilidade da emulsão (David Julian McClements, 2015; Guida; Aguiar; Cunha, 2021; Kalashnikova et al., 2013; Lu; Tian, 2021a; Mcclements; Jafari, 2017). As emulsões mais clássicas se dão pela mistura de óleo em água, os emulsificantes dispersam as moléculas de óleo na água em forma de gotas ou glóbulos. Emulsificantes são moléculas anfipáticas, ou seja, possuem uma extremidade polar e outra apolar, que podem ser quimicamente sintetizados (como os polissorbatos) ou de origem animal (como proteínas do leite, carne e ovos). A extremidade polar do emulsificante, por afinidade, fica em contato com a água, enquanto a extremidade apolar fica no interior da gota de óleo. (David Julian McClements, 2015; Franzol; Rezende, 2015; Lv et al., 2021).

Mais recentemente, muitos consumidores têm se conscientizado das consequências éticas e ambientais que os produtos contendo emulsificantes sintéticos (surfactantes) podem causar. Essa abordagem atende ao perfil de consumo, que tem se modificado nos últimos anos, privilegiando produtos com rótulos mais limpos, os chamados *clean label* (Guida; Aguiar; Cunha, 2021; McClements; Bai; Chung, 2017). Uma alternativa ao uso de emulsões tradicionais são as emulsões Pickering, que são emulsões estabilizadas por partículas coloidais, muito aplicadas em indústrias farmacêuticas, alimentícias e cosméticas.

Durante o processo de homogeneização as partículas coloidais se acumulam na região de interface entre as micelas de óleo e a água formando uma barreira física (Lu; Xiao; Huang, 2018; Zhu, 2019). Essas emulsões são mais estáveis do que as tradicionais, devido ao revestimento das gotículas por partículas sólidas, que funciona como uma rígida barreira mecânica contra coalescência, aumentando, assim, a estabilidade da emulsão. Essas partículas sólidas devem, preferencialmente, ser derivadas de fontes naturais e abundantes, dispensando o uso de surfactantes em sua composição. A ausência de surfactantes favorece a formulação de produtos para os quais seu uso tem efeitos negativos, tais como irritação, citotoxicidade e comportamento hemolítico, podendo ter aplicações em produtos farmacêuticos, liberação controlada de substâncias, cosméticos e sistemas de encapsulamento (Asabuwa Ngwabebhoh; Ilkar Erdagi; Yildiz, 2018; Berton-Carabin; Schroën, 2015; Chevalier; Bolzinger, 2013; Sarkar

et al., 2019; Winuprasith et al., 2018). Uma alternativa de partículas sólidas, bastante explorada e promissora, para composição de uma emulsão Pickering sustentável é o amido.

O amido é um dos principais polissacarídeos do planeta, é uma molécula natural e abundante que pode ser extraída de diversas plantas, como banana, manga, milho e batata (Zia-ud-Din; Xiong; Fei, 2017). O amido é um polímero organizado em uma estrutura de dupla hélice e seus principais componentes são a amilose e a amilopectina. A amilose, formada por unidades de glicose unidas por ligações glicosídicas α -1,4, origina uma cadeia linear e a amilopectina, formada por unidades de glicose unidas em α -1,4 e α -1,6, forma uma estrutura ramificada. As proporções em que essas estruturas aparecem no amido variam de acordo com a fonte de origem do amido (Bangar et al., 2023; Le Corre; Bras; Dufresne, 2010). Esses dois polímeros criam uma estrutura semicristalina que resulta em diferentes tamanhos de grânulos de amido, variando de 0,5 a 175 μ m, dependendo da fonte do amido (Lu; Tian, 2021a; Zia-ud-Din; Xiong; Fei, 2017). O uso de nanopartículas de amido (nanoamido) tem sido estudado para uso em soluções filmogênicas, aerogeis e emulsões. O nanoamido se mostra como uma partícula promissora para ser usada na estabilização de emulsões Pickering devido sua elevada área superficial, não toxicidade, biodegradabilidade e biocompatibilidade (Apriyanto; Compart; Fettke, 2022; Han et al., 2022; Marto et al., 2019).

Convencionalmente, o nanoamido é obtido por meio da hidrólise ácida dos grãos de amido. O ácido é o responsável por degradar a parte amorfa da estrutura do amido restando assim uma estrutura de tamanho reduzido e com alta cristalinidade (Lu; Tian, 2021a; Mohammad Amini; Razavi, 2016; Wang et al., 2022). Entretanto, rotas físicas de desconstrução para o amido têm sido cada vez mais buscadas e estudadas, como, por exemplo, a moagem (Bangar et al., 2023; Lu; Xiao; Huang, 2018; Tamaki et al., 1998)

O uso de moinho de bolas é um método seguro e econômico de desconstrução de partículas com baixa/nula geração de resíduos e que já é bastante aplicado em processos da indústria alimentícia. O amido, quando modificado pelo moinho de bolas, tem sua estrutura cristalina danificada pela ação combinada da fricção, colisão e cisalhamento, causados pelo choque entre as bolas e o choque contra as paredes do moinho, resultando em partículas significativamente menores e com propriedades finais distintas a do amido in natura, com foco especial na temperatura de gelatinização (Barros et al., 2023; Liu et al., 2013; Lu; Tian, 2021a).

Para a obtenção de um nanoamido moído de grau alimentício, e modificado para garantir uma maior estabilidade quando aplicado à uma emulsão Pickering, muitos trabalhos utilizam a moagem de bolas associada à oxidação com anidrido 2-octen-1-ilsuccínico (ASO), que é um

procedimento aprovado pelo Food and Drug Administration (FDA); mas que, apesar de seguro para consumo, ainda produz resíduos durante o processo que precisam ser devidamente descartados para que não causem danos ao meio ambiente (Agama-Acevedo; Bello-Perez, 2017; Dokić; Krstonošić; Nikolić, 2012; Liu et al., 2018a).

A quitina, outro polímero natural e amplamente disponível, pode ser obtida dos exoesqueletos de caranguejos, lagostas e outros crustáceos, assim como da parede celular de fungos, como cogumelos. Quando convertida em nanofibras ou nanocristais, a quitina se revela como uma excelente partícula para a estabilização de sistemas coloidais, uma vez que seus grupos aminos concedem a esse material uma elevada carga positiva que favorece a estabilização de sistemas coloidais por repulsão eletrostática. (Huan et al., 2021; Jones et al., 2020). Além disso, a quitina exibe propriedades antibacterianas e antifúngicas devido à presença de vários grupos amino (NH₂) em sua cadeia. Quando utilizada como revestimento em gotas de óleos, ela reduz a digestão lipídica no organismo, o que é particularmente interessante para aplicações biomédicas e alimentícias (Jiménez-Saelices et al., 2020; Lv et al., 2021; Zhou et al., 2021).

Assim, a combinação das propriedades vantajosas do amido, como baixo custo, fácil digestibilidade e biocompatibilidade, com as da quitina, incluindo propriedades antibacterianas, carga positiva e melhorias na absorção de óleo, emerge como uma abordagem promissora para a estabilização de emulsões Pickering. Essa estratégia não apenas reduz os custos em comparação com uma emulsão contendo apenas quitina, tendo em vista que a diferença de valores desses polissacarídeos pode ser de até 300% em revendedores como a Sigma-Aldrich, mas também melhora a estabilidade por meio de cargas, sem a necessidade de solventes orgânicos, diferentemente de uma emulsão de amido.

O desenvolvimento de emulsões de Pickering de grau alimentício baseadas em biopolímeros naturais está alinhado com múltiplos Objetivos de Desenvolvimento Sustentável (ODS) das Nações Unidas, como o ODS 3 (Saúde e Bem-Estar), ODS 12 (Consumo e Produção Responsáveis) e ODS 13 (Ação Contra a Mudança Global do Clima). Ao substituir surfactantes sintéticos por materiais biodegradáveis e renováveis obtidos de resíduos agroindustriais (por exemplo, amido proveniente de desperdício de alimentos, quitina de subprodutos de frutos do mar), esses sistemas promovem a saúde, reduzem o impacto ambiental e contribuem para uma economia circular (United Nations, 2015).

Dito isto, o presente trabalho aborda a obtenção de partículas de amido por meio de moagem e o estudo do efeito do moinho em suas propriedades e o uso dessas partículas juntamente com nano cristais de quitina para a estabilização de emulsões Pickering.

Esse documento é dividido em capítulos como descrito abaixo:

Capítulo 1: Este capítulo apresenta uma revisão da literatura que contextualiza os temas discutidos nos capítulos 2 e 3.

Capítulo 2: Este capítulo apresenta o artigo científico “Effect of ball-milling on starch crystalline structure, gelatinization temperature, and rheological properties: towards enhanced utilization in thermosensitive systems” publicado em 2023 na revista Foods do MDPI. *Foods* 2023, 12(15), 2924; <https://doi.org/10.3390/foods12152924>.

Capítulo 3: Este capítulo apresenta o artigo científico “Optimizing Pickering emulsion stability: unveiling the synergistic potential of starch nanoparticles and chitin nanocrystals” submetido para publicação em 2025 na revista Carbohydrate Polymers da Elsevier.

2 OBJETIVOS

2.1 Objetivo Geral

Obter nanopartículas de amido por rota mecanoquímica e utilizá-las para desenvolver emulsões Pickering o/w estabilizadas com partículas de amido e nano quitina.

2.1 Objetivos Específicos

Determinar as melhores condições de obtenção de nanopartículas de amido por meio de moagem;

Determinar o efeito da moagem nas características do nanoamido obtido como temperatura de gelatinização;

Determinar o efeito da combinação de nanopartículas de amido e nano quitina na estabilização de emulsões Pickering;

Determinar o efeito da gelatinização do amido na estabilização de emulsões Pickering.

3 LITERATURE REVIEW

3.1 Problem Statement and Context

Traditional emulsion systems are widely used in food products, which are largely present in our day-to-day life, like yogurt, milk, salad dressings, dips, desserts, etc. The stabilization of emulsions within complex food matrices presents significant challenges, largely due to intricate interfacial phenomena occurring between the immiscible aqueous and oil phases. Most of the food products currently in market are stabilized by a synthetic emulsifier which aren't always the best option when it comes to biocompatibility and health benefits (Zhu et al., 2021).

Synthetic surfactants, while historically prevalent, exhibit some limitations in food applications. These include potential cytotoxicity, environmental burden due to bioaccumulation or improper waste management, and adverse impacts on organoleptic properties through interactions with flavor compounds and texturizing agents (Bai et al., 2021; Cabrita et al., 2023).

Furthermore, synthetic emulsifiers rapidly adsorb onto droplet surfaces and exist in dynamic equilibrium with their non-adsorbed form. This behavior reduces the interfacial tension, making droplets more susceptible to deformation, disruption, and potentially coalescence (Cui et al., 2021b). Moreover, their derivation from mostly non-renewable sources is increasingly incompatible with the principles of sustainability and the growing consumer demand for clean-label, minimally processed products (Bai et al., 2021; Berton-Carabin; Schroën, 2015; Zhu et al., 2021).

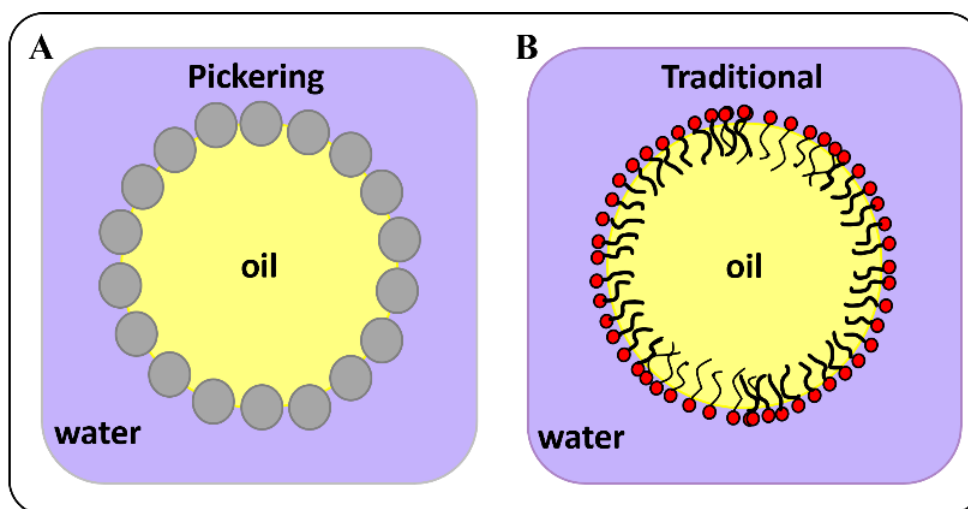
Consequently, there has been increasing research into the use of naturally sourced emulsifying agents. Plant- and microbe-derived biosurfactants represent alternatives due to their biodegradability and perceived safety (Ehsani et al., 2018; Thraeib et al., 2022; Yang et al., 2025). Similarly, the use of animal-derived proteins, although effective as emulsifiers, is increasingly constrained by ethical, dietary, and allergenic considerations (McClements; Lu; Grossmann, 2022).

In this context, polysaccharides and their derivatives have emerged as highly promising candidates for stabilizing emulsions, the emulsions stabilized by solid particles like polysaccharides are called Pickering emulsions (Chevalier; Bolzinger, 2013; Liu et al., 2024b; Xu et al., 2020).

3.2 Pickering Emulsions

Pickering emulsions are a distinct class of emulsions stabilized not by traditional molecular surfactants, but by solid colloidal particles adsorbed at the oil/water interface. First described in the early 20th century by S. Pickering (1907), these systems differ fundamentally from classical emulsions in their stabilization mechanism and structural characteristics. In Pickering emulsions, the solid particles form a robust interfacial layer around dispersed droplets, creating a steric barrier that impedes coalescence and enhances kinetic stability (Figure 1). Particle emulsifiers, typically partially wetted by both oil and water phases, tend to adsorb slowly and irreversibly onto the interface, without significantly reducing interfacial tension. This structure provides exceptional resistance to destabilizing processes such as Ostwald ripening and phase separation (Cui et al., 2021b; Pickering, 1907).

Figure 1 – Schematic representation of a droplet in a Pickering emulsion (A) and a traditional emulsion (B)



Source: Made by the author.

The physicochemical properties of the particles play a central role in determining the stability and performance of Pickering emulsions. To act effectively as Pickering stabilizers, particles must possess specific properties, including: (a) partial wettability (contact angle at the oil-water interface between 15° – 90°), (b) nanoscale size (ideally 50–500 nm), (c) sufficient surface charge to ensure electrostatic stabilization, and (d) mechanical rigidity to form stable interfacial layers. Surface functional groups and roughness also contribute to their interfacial behavior (Keramat; Kheynoor; Golmakani, 2022; Yang et al., 2025). Smaller particles can

cover a greater interfacial area, which is advantageous for forming stable emulsions, although this might require higher particle concentrations. Surface charge influences electrostatic interactions among particles and affects their dispersion in the continuous phase, thereby impacting emulsion homogeneity and stability. Optimization of these properties is essential to achieve desired functionalities, particularly for applications in food systems where processing conditions such as pH, temperature, and shear may vary (Cui et al., 2021a).

In the context of sustainable and functional food development, the use of biopolymer-based stabilizers has gained momentum. These materials, derived from renewable sources, are generally recognized as safe (GRAS) and are valued for their biodegradability, biocompatibility, and regulatory acceptability. Biopolymers must be capable of adsorbing at interfaces and providing steric and/or electrostatic stabilization under processing conditions. Among natural candidates, proteins and polysaccharides have emerged as leading classes of stabilizers. Proteins such as whey protein isolate, zein, and various plant-derived proteins can form nanoscale aggregates with amphiphilic properties, enabling them to adsorb at interfaces and stabilize emulsions. However, their performance can be sensitive to environmental factors such as pH and ionic strength (Liu et al., 2024a; McClements; Lu; Grossmann, 2022; Mwangi et al., 2020).

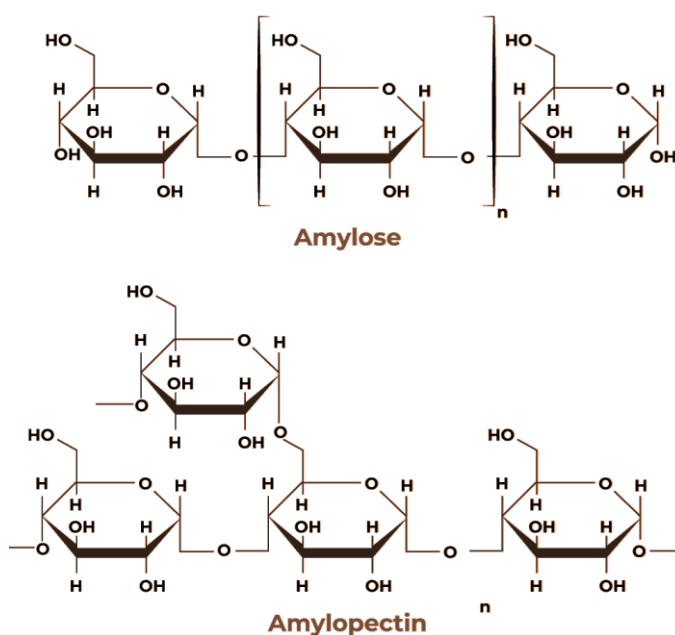
Polysaccharides offer a plethora of structures and functionalities, making them highly versatile as Pickering stabilizers. Cellulose, typically used in the form of nanocrystals (CNCs) or nanofibrils (CNFs), provides high mechanical strength and surface area, forming rigid, rod-like particles that create robust interfacial networks (Bai et al., 2019). Starch nanocrystals (SNCs), derived from abundant and low-cost sources, have tunable surface properties and show promising results in emulsion stabilization (Ko; Kim, 2021). Chitin and its deacetylated derivative chitosan due to their high positive charge are great at stabilizing colloidal systems (Lv et al., 2021). These are but a few of the polysaccharides that can be used as particles for Pickering emulsion stabilization, other examples are pectin and gum arabic (Cui et al., 2021b).

The incorporation of these biopolymer-based particles into Pickering emulsions not only supports the development of environmentally friendly and clean-label food products but also enables novel functionalities such as controlled release of bioactives, improved textural properties, and enhanced nutritional profiles (Asabuwa Ngwabebhoh; Ilkar Erdagi; Yildiz, 2018; Yang et al., 2025). Continued research into the nanoengineering and functionalization of biopolymer particles is expected to further advance their performance and expand their applicability in complex food systems

3.3 Starch Nanoparticles

Starch is a naturally abundant, biodegradable, and renewable polysaccharide widely used in the food industry. It is composed of two main glucose polymers: amylose, which is mostly linear with $\alpha(1\rightarrow4)$ linkages, and amylopectin, a highly branched polymer containing both $\alpha(1\rightarrow4)$ and $\alpha(1\rightarrow6)$ linkages (Figure 2). Amylose is predominantly linear with $\alpha(1\rightarrow4)$ glycosidic bonds, while amylopectin has a branched structure with both $\alpha(1\rightarrow4)$ and $\alpha(1\rightarrow6)$ linkages. This structural complexity influences the gelatinization, retrogradation, and digestibility of starch, which can be critical when designing nanoparticles for emulsion stabilization. Moreover, native starch granules possess a semi-crystalline structure, typically composed of alternating amorphous and crystalline regions, and vary in shape and size depending on the botanical source. This granular architecture must often be disrupted to produce effective nanoparticulate stabilizers. (Leal-Lazareno et al., 2025). However, native starch granules are often too large and lack the surface activity and wettability required for effective adsorption at oil/water interfaces. Thus, modification of starch structure is used as a strategy to enhance its interfacial functionality and enable its application in emulsion stabilization (Lu; Xiao; Huang, 2018).

Figure 2 – Chemical structures of amylose and amylopectin.



Source: Made by the author.

For Pickering stabilization, starch must be processed into smaller, nanoscale particles, such as starch nanocrystals (SNCs), that can effectively adsorb at droplet interfaces and form a stabilizing barrier. These particles must possess a balanced hydrophilic-hydrophobic character and sufficient surface charge or roughness to create a steric or electrostatic barrier against coalescence (Lu; Xiao; Huang, 2018; Xu et al., 2023).

Several methods have been developed to reduce starch particle size and tailor surface properties for use in Pickering emulsions like, acid hydrolysis, enzymatic treatment and physical methods.

The hydrolysis makes use of strong acids (e.g., HCl or H₂SO₄) to remove amorphous regions of the starch granule, yielding nanocrystalline particles with enhanced rigidity and surface area (Lu; Tian, 2021a; Marta et al., 2023). On the other hand, enzymes such as α -amylase or pullulanase can break down specific linkages in the starch molecule, allowing for controlled particle size reduction and potentially preserving more natural characteristics compared to chemical methods, but this process can prove to be quite costly (Apriyanto; Compart; Fettke, 2022; Park; Kim, 2021). Lastly, physical approaches like ultrasonication, high-pressure homogenization, or milling techniques can mechanically reduce starch granules to nanoscale dimensions, often used in combination with chemical or enzymatic steps for improved efficiency (Bangar et al., 2023; Barros et al., 2023; Park; Kim, 2021).

Previous studies have demonstrated that starch-based nanoparticles can effectively stabilize Pickering emulsions. However, many of these applications rely on chemical modifications, such as esterification, to improve hydrophobicity and interfacial activity. While effective, such modifications may conflict with clean-label and natural formulation goals (Wang et al., 2022; Xu et al., 2023).

To address this limitation, recent research has explored the combination of biopolymers as an alternative strategy. For example, pairing starch, chitin or cellulose nanocrystals with other naturally derived colloidal particles. This approach not only enhances emulsion stability without the need for chemical modification but also supports the development of multifunctional systems with improved environmental compatibility and consumer acceptance (Cui et al., 2021b; Lv et al., 2021; Xu et al., 2023).

3.4 Chitin Nanocrystals

Chitin nanocrystals (ChNCs) have emerged as promising candidates for stabilizing Pickering emulsions, particularly in food systems seeking sustainable, multifunctional, and biocompatible alternatives to conventional emulsifiers. Chitin is the second most abundant biopolymer in nature, primarily found in the exoskeletons of crustaceans (e.g., shrimp, crab), as well as in the cell walls of fungi and some insects. The nanocrystalline form of chitin is obtained through controlled depolymerization processes, via hydrolysis, that preserve its crystalline domains while removing amorphous regions (Jones et al., 2020; Larbi et al., 2018; Sara et al., 2019).

The extraction of chitin nanocrystals typically begins with the isolation of bulk chitin, which involves deproteinization and demineralization steps to remove associated proteins and calcium carbonate from the biological sources. Once purified, chitin is subjected to acid hydrolysis, usually with hydrochloric or sulfuric acid, to selectively degrade amorphous regions and release rod-like nanocrystals with high crystallinity and defined aspect ratios (Larbi et al., 2018; Su et al., 2024).

ChNCs typically exhibit lengths ranging from 100 to 500 nm and diameters below 50 nm, depending on the source and processing conditions. Chitin's inherent properties, such as its semicrystalline structure, hydrogen bonding capacity, and limited solubility, are significantly altered upon nanocrystal formation. The resulting chitin nanocrystals exhibit increased surface area, mechanical strength, and a high density of reactive groups, particularly protonated amino groups in acidic media. These changes enhance their colloidal stability, interfacial activity, and functional performance in Pickering emulsions (Muñoz-Núñez; Fernández-García; Muñoz-Bonilla, 2022).

Chitin nanocrystals offer several intrinsic advantages for Pickering stabilization. Their high aspect ratio and strong surface charge enable efficient adsorption at oil/water interfaces, forming rigid interfacial layers that resist droplet coalescence. In addition, their amphiphilic nature, arising from alternating hydrophilic (hydroxyl, amino) and hydrophobic (acetyl) groups, supports partial wettability, a key requirement for effective stabilization (Paredes-Toledo et al., 2025).

Unlike many traditional stabilizers, ChNCs provide electrostatic stabilization and steric hindrance simultaneously, making them highly effective even at low concentrations. Their positive surface charge also complements negatively charged particles (e.g., cellulose

nanocrystals), opening opportunities for synergistic combinations in hybrid Pickering systems (Facchine et al., 2021; Zhou et al., 2020a).

In food systems, chitin nanocrystals not only act as physical stabilizers but also contribute functional bioactivity, most notably antimicrobial properties. This is particularly relevant in emulsified food products where microbial growth at oil/water interfaces can be problematic. The antimicrobial activity of ChNCs, attributed to their cationic nature and ability to interact with microbial membranes, adds value to formulations aiming for extended shelf life and reduced use of synthetic preservatives. Moreover, ChNCs are non-toxic, biodegradable, and derived from renewable sources, aligning well with current industry trends toward clean-label and environmentally friendly products (Facchine et al., 2021; Guo et al., 2023; Zhou et al., 2020b).

3.5 Pickering applications in Food Systems

The integration of Pickering emulsions into food systems presents a compelling strategy to overcome the limitations of conventional emulsions, particularly in terms of stability, safety, and sustainability. Traditional emulsions often suffer from instability due to surfactant desorption, droplet coalescence, and sensitivity to environmental factors. Moreover, concerns related to the toxicity and environmental impact of synthetic emulsifiers have accelerated the search for natural, food-grade alternatives (Azfaralariff et al., 2020; Bai et al., 2021).

Pickering emulsions stabilized by biopolymers such as cellulose, starch and chitin nanocrystals offer a versatile platform for functional formulations, including the encapsulation of sensitive bioactive compounds (e.g., essential oils, vitamins, probiotics). Their biocompatibility and biodegradability make them highly suitable for food and nutraceutical applications. The rigid, particle-based interfacial layer not only protects encapsulated actives from degradation but also facilitates controlled release and targeted delivery in the gastrointestinal tract (Mwangi et al., 2020; Ye; Georges; Selomulya, 2018). For example, Pickering emulsions have been successfully applied in salad dressings, mayonnaise analogues, and dairy alternatives, offering improved oxidative stability, texture, and shelf life without synthetic emulsifiers (Ji; Wang, 2025; Ma et al., 2025; Narciso et al., 2025).

In addition, Pickering emulsions exhibit superior stability under real processing and storage conditions. Compared to surfactant-based systems, they are more resistant to environmental stresses such as pH fluctuations, high temperatures, and varying ionic strength,

conditions frequently encountered in food manufacturing. This enhanced robustness is largely attributed to the irreversible adsorption of solid particles at the droplet interface, creating a durable physical barrier against coalescence (Lv et al., 2021; Yang et al., 2025).

From a product development perspective, Pickering emulsions align strongly with current trends in the food industry, including the demand for clean label, plant-based, and functional foods. Their ability to eliminate or reduce the need for synthetic additives appeals to health-conscious consumers, while their natural origin and potential for zero-waste sourcing (e.g., chitin from crustacean shells) contribute to circular economy initiatives (Bai et al., 2021; Berton-Carabin; Schroën, 2015).

These features position Pickering emulsions as a transformative technology for the next generation of food products, offering not only enhanced physical performance but also added nutritional and environmental value. Ongoing research into hybrid systems, combining different biopolymers or incorporating bioactive functionalities, is expected to further expand their applicability across a wide range of food and beverage categories (Ji; Wang, 2025; Ma et al., 2025; Narciso et al., 2025; Zhou et al., 2020a).

4 EFFECT OF BALL-MILLING ON STARCH CRYSTALLINE STRUCTURE, GELATINIZATION TEMPERATURE, AND RHEOLOGICAL PROPERTIES: TOWARDS ENHANCED UTILIZATION IN THERMOSENSITIVE SYSTEMS

<https://doi.org/10.3390/foods12152924>

Abstract

Starch's crystalline structure and gelatinization temperature might facilitate or hinder its use. Ball-milling has frequently been mentioned in the literature as a method for reducing starch size and as a more environmentally friendly way to change starch, such as by increasing surface area and reactivity, which has an impact on other starch properties. In this study, starch samples were milled for varying durations (1, 5, 10, 20, and 30 h) and at different starch-to-ball mass ratios (1:6 and 1:20). Microscopy and XRD revealed that prolonged milling resulted in effective fragmentation and a decrease in crystallinity of the starch granules. Increasing milling times increased amylose content. Rheology and thermal studies revealed that gelatinization temperatures dropped with milling duration and that viscosity and thixotropy were directly influenced. The sample milled for 10, 20, and 30 h at a ratio of 1:20 were the most fragmented and upon drying formed a trans-parent film at ambient temperature, because of the lower gelatinization temperature. Starch ball milling could lead to the use of this material in thermosensitive systems.

Keywords: Ball-milling; Corn starch; Gelatinization temperature.

4.1 Introduction

Starch, a biopolymer and one of the main polysaccharides on the planet, is a natural and abundant molecule extracted from various plants, such as but not limited to cassava, corn, and potatoes (Zia-ud-Din; Xiong; Fei, 2017). Anhydroglucose forms a linear chain structure linked by glycosidic linkages (α 1-4). These linear chains link with each other, forming amylose (AM) and amylopectin (AP). Together, AM and AP form alternating crystalline and amorphous lamellae, which are arranged into growth rings originating from the hilum, forming the starch granule (Han et al., 2022; Li; Dhital; Hasjim, 2014).

Starch's main components (amylose and amylopectin) have entirely different properties. Amylose, a macromolecule formed by glucose units joined by α -1,4 glycosidic bonds, gives rise to a primarily linear chain with a few long ramifications. Amylopectin, formed by glucose units joined by α -1,4 and α -1,6 glycosidic bonds, creates a smaller, highly branched structure that is organized in a double helix conformation. As a result, amylose tends to retrograde, producing tough gels and strong films, while amylopectin dispersed in water forms soft gels and ductile films (Pérez; Bertoft, 2010). Due to its structured chains, amylopectin is more influential in the crystallinity of the starch granule than amylose, which is usually related to the amorphous region of the granule. A higher amylose content is associated with lower plasticization and gelatinization temperatures. The proportions in which these structures appear in starch vary according to the source (Apriyanto; Compart; Fettke, 2022; Le Corre; Bras; Dufresne, 2010). These two components create a semicrystalline structure that results in different crystallinities and assorted sizes of starch granules, ranging from 0.5 to 175 μm , depending on the starch source (Lu; Tian, 2021a; Zia-ud-Din; Xiong; Fei, 2017).

The scope of starch application in its natural form is enhanced and limited due to its unique structure. For example, when in water and subjected to heating (60 – 90 °C), it forms a viscous paste that becomes a brittle gel after cooling, which can be desirable or not, depending on the final application. Another example of its unique structure influencing the application is its semicrystalline organization. The compact molecules in the crystalline region inhibit water and other chemicals from accessing and reacting with the molecules in this region, increasing the gelatinization temperature and decreasing the starch chemical reactivity (Huang et al., 2008). Several studies have modified starch using chemicals (hydrolysis, oxidation, etc.) and enzymes to improve properties such as reactivity and surface area and enable the application of this material in different sectors, such as suspension stabilizers, thermoplastic starch, packaging, etc. (Chakraborty et al., 2022; Torres; De-la-Torre, 2022; Wang et al., 2022).

A greener route to modify starch would be the milling process, as it is a process that generates no residues that could harm the environment, unlike hydrolysis, for example, which uses acids and/or organic solvents. Starch milling is widely reported in the literature as a technique for reducing the size of starch granules and ensures higher safety, simplicity and cost-efficiency compared to other treatments. Ball-milling performs the partial breakdown of the starch structure through friction, impact, and shear, caused by the collision of the balls with the starch and the starch with the mill wall, increasing the surface area and reactivity and reducing the granule size of the starch (Liu et al., 2018b). However, this reduction in the size of the

granules and partial breakdown of the crystalline structure of the starch may reflect a change in other properties, such as the level of chain organization, crystallinity, and amylose content. Additionally, ball milling is reported to directly affect the starch granules surface area (Bangar et al., 2023; Lu; Tian, 2021a; Tamaki et al., 1998).

As a result, this research aims to study the thermal and rheological characteristics of these starches by using ball-milling processing, which affects the granule surface area, as a greener way to alter starch properties, particularly its gelatinization temperature, and determine the structural changes affected by milling time (1, 5, 10, 20, and 30 h). Further considerations on possible applications for the obtained starches are discussed.

4.2 Materials and Methods

4.2.1 Corn starch

This work used commercially available food-grade corn starch (Kimimo, Brazil) as feedstock, with a humidity content of ~ 11%.

4.2.2 Starch ball milling

A ceramic ball mill (20 cm diameter) with ceramic balls (1.5 cm) was used with two different starch/ball mass ratios, 1:6 and 1:20 (Huang et al., 2008; Liu et al., 2018a). Operation was performed at room temperature (30 °C) and 230 rpm for 1 h, 5 h, 10 h, 20 h and 30 h.

4.2.3 Microscopy analysis

For scanning electron microscopy (SEM), starch samples were mounted in stubs, covered with a thin layer of gold in a metallic covering device (Emitech, model K550), and visualized under a voltage acceleration of 15 kV in different increments on a Quanta 450-FEG, FEI.

Light microscopy analysis was performed to observe the Maltese cross in the starch granules using an optical microscope with polarized light. Samples of starch (0.01 g) were added to 1 mL of a glycerol solution (50% m/v), and 0.5 mL of this suspension was transferred to a microscope slide and covered with a coverslip for visualization under polarized light.

4.2.4 Fourier transform infrared spectroscopy (FTIR)

The spectra of the starch samples were obtained using a PerkinElmer® Spectrum Two spectrometer (PerkinElmer, USA) with a resolution of 4 cm^{-1} , wavelength range from 4000 to 600 cm^{-1} , and 32 scans. The starch spectra were obtained via the attenuated total reflection (ATR) method.

The effect of ball milling on the ordered structure of the starch was also evaluated using FTIR spectra. It has been reported that bands between 950 and 1100 cm^{-1} are sensitive to changes in the starch structure, especially those at approximately 995 and 1044 cm^{-1} , where the first is commonly related to the amorphous structure of the starch and the latter to the ordered structure of the starch (Goiana et al., 2021; Pozo et al., 2018). Therefore, the 995:1044 cm^{-1} intensity ratio was used to indicate the degree of order in the starch structure.

4.2.5 Amylose content

The amylose content was determined based on the methodology proposed by Chrastil et al. and Hu et al. (Chrastil, 1987; Hu et al., 2016), with modifications. In test tubes, 0.1 g of starch, 1.0 mL of absolute ethanol, and 10 mL of a solution of sodium hydroxide (1 M) were added. The tubes were heated in a water bath (70 °C – 15 min), shaken at 5 min intervals, and then cooled to room temperature in a cold-water bath. In a 50 mL beaker, 0.5 mL of the solubilized starch, 2.0 mL of iodine solution ($\text{I}_2 + \text{KI}$; 0.01 M), 1.0 mL of acetic acid solution (1 M), and 46 mL of distilled water were added. This solution reacted at room temperature for 10 min. The absorbance reading was performed in a spectrophotometer (Shimadzu) at 620 nm using an acrylic cuvette with 1.4 mL of a starch solution with iodine and acetic acid and 1.4 mL of distilled water, and the absorbance was compared with the calibration curve. The blank reading was carried out using only distilled water.

4.2.6 Thermogravimetric analysis (TGA)

Thermogravimetric measurements were performed using starch samples (~ 10 mg) in a PerkinElmer® TGA 6000 instrument with temperatures ranging from 50 to 600 °C, a heating rate of 10 °C/min, under a nitrogen atmosphere with a flow of 40 mL/min.

4.2.7 Differential scanning calorimetry (DSC)

DSC analysis was performed in a TA Instruments DSC (model Q20) with a hermetic aluminum pan. The pans were hermetically sealed after being filled with approximately 1.5 mg of the starch sample and 5 μ L of distilled water. The temperature ranged from 30 to 100 °C, with a heating ramp of 10 °C/min, and the experiment was carried out in a nitrogen atmosphere.

4.2.8 X-ray diffraction (XRD)

The DRX diffraction graphs were produced using a Co tube at 40 kV and 40 mA with a diffractometer for polycrystalline samples, model XpertPro MPD - Panalytical. The sweep speed was 0.5°/min, and the 2-theta angle ranged from 5 to 40°. Diffractogram deconvolution was performed, and the Crystallinity Index (CrI), which measures the proportion of crystalline peak regions to all deconvoluted peaks, was determined using the equation below (Eq. 1).

$$CrI = \frac{\text{crystalline region area}}{\text{total area}} \quad (1)$$

4.2.9 Swelling power (SP) and Solubility (S%)

SP and S% were calculated using a modified version of the approach described by Fu et al. and Mandala et al. (Fu et al., 2012; Mandala & Bayas, 2004). A centrifuge tube with a screw lid was filled with 0.4 g (W₀) of the starch samples. After adding distilled water to achieve a final starch concentration of 2.0% (w/w), the tubes were vortexed at room temperature (25 °C). Finally, the tubes were centrifuged for 15 min at 1006 g. The supernatant was carefully drained off in a petri dish, and the residue weight was noted (W_p). The tubes with the residue and the petri dishes with the supernatant were dried in an air oven (105 °C) until constant weight (W_d and W_s, respectively). The swelling power (SP) and the Solubility (S%) of the samples were calculated using the equations below (Eq. 2 and Eq. 3).

$$SP = \frac{W_p}{W_d} \quad (2)$$

$$S\% = \left(\frac{W_s}{W_0} \right) \cdot 100 \quad (3)$$

4.2.10 Rheology

Rheological studies were conducted in the linear viscoelastic zone of the samples using a Thermo Scientific rheometer (HAAKE MARS). The samples for gelatinization temperature were prepared by making a 5% (w/w) starch suspension and using a gelatinized starch solution (5% starch in water heated at 90 °C for 10 min), as a 5% gelatinized starch solution is more viscous than water, the starch solution was employed in place of water to reduce the effects of starch precipitation. The samples for viscosity (oscillatory rheology experiment) and thixotropy analysis were prepared by heating to 90 °C for 10 min in a 5% suspension of the starch samples in distilled water.

An oscillatory rheology experiment was performed for 2 min at 25 °C and 1% deformation using a cone plate geometry with a gap of 0.05 mm (C60/1-TiL) to estimate the dynamic viscosity, storage module (G'), and loss module (G'') of the samples. The same measuring geometry was used for gelatinization temperature measurements in a rotational experiment with a 1 s^{-1} shear rate and a heating rate of 7.2 °C/min from 30 to 75 °C. The gelatinization temperature was defined as the temperature at which the sample began to undergo a sudden change in viscosity.

The thixotropy measurements were performed in a rotational experiment utilizing the previously described geometry. The shear rate was increased linearly from 0.1 to 10 s^{-1} in 120 s and then held constant at 10 s^{-1} for 30 s before decreasing (linearly) to 0.1 s^{-1} in 120 s. The areas of thixotropy (defined as work performed for the demolition and reconstruction of a sample inner structure) were computed by adding the areas of certain trapeziums between the curves "up" and "down".

4.2.11 Film forming ability

For the film forming ability assays, milled starch aqueous suspensions (10%, w/w) were prepared at room temperature, subsequently poured into Petri dishes, and then dried for 16 h in a vacuum oven at 30 °C. The resulting films were registered with pictures to observe the effect of milling on the starch film forming capacity at low temperatures.

4.2.12 ANOVA Analysis

The statistical analysis was performed using the analysis of variance produced with the software Statistica10 (StatSoft, Tulsa, OK, USA). Tukey's test was applied to detect significant differences; $p < 0.05$ was considered statistically significant.

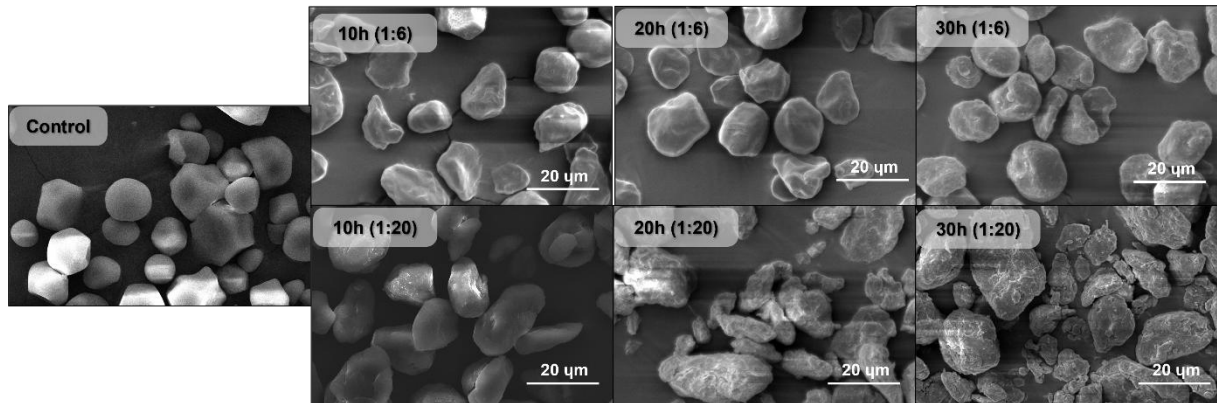
4.3 Results and discussion

4.3.1 Microscopic analysis

The microscopic images obtained via SEM showed that the starch granule was fractured throughout the ball-milling process (Figure 3). The effects of the ball-milling process are visible in the images as the milling time increases due to the breakdown of the granules through impact, friction, and shear forces. It is important to note that there is a slight increase in the system's temperature as the milling proceeds (37 °C at the end of the process). This increase must not have had a significant impact on the process of breaking the granules. The starch granules were oval shaped with a smooth surface. However, as the milling time increases, the surface becomes rougher, and the granule is broken down, as evidenced by the appearance of fractures of varying sizes and shapes (Han et al., 2022).

The most fractured and heterogeneous group of granules was shown by the starch milled using the 1:20 starch/ball ratio. However, the particle size does not always decrease with milling time due to the agglomeration of the damaged starch granules. This agglomeration can be undone by suspending the starch in some solvent if the application of the material calls for it (Bangar et al., 2023; Li; Dhital; Hasjim, 2014; Zia-ud-Din; Xiong; Fei, 2017). This fractured structure of the ball-milled starch gives it a larger surface area. Consequently, its reactivity increases since it is now easier for water and other chemicals to access the middle of the granule through the fractures formed during the milling process (Liu et al., 2018b; Lu; Tian, 2021a).

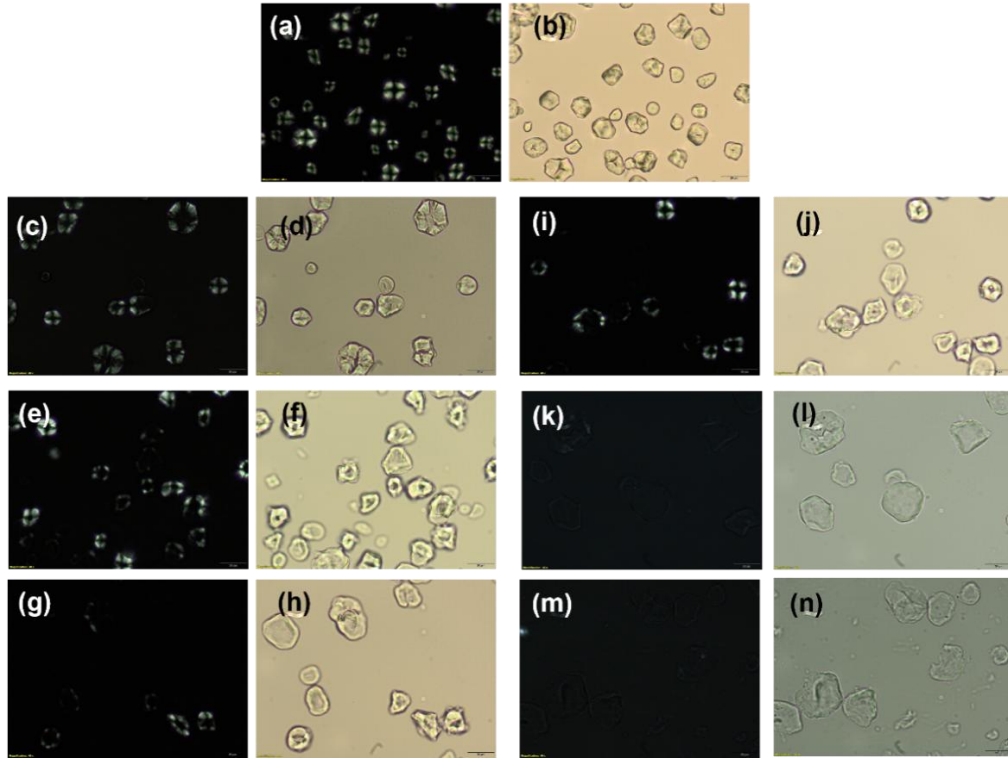
Figure 3 – Scanning electron micrographs of starch, both control and milled samples. Scale bars: 20 μm .



Source: Made by the author.

The light microscopy analysis of the control starch clearly showed birefringence (Figure 4), which is correlated to the crystalline structure of the starch granule (Shi; Sweedman; Shi, 2021). However, as the milling time increases, the birefringence starts to fade, with complete fading in the conditions using 1:20 ratios. The complete disappearance of the birefringence indicates that the crystalline structure of the starch granules was fractured entirely, leaving a less organized amorphous structure in its place. The milling process not only superficially fractured the granule but also broke down the starch crystalline region, and this outcome might be improved further by adopting a more powerful ball mill capable of running at a higher rpm, reducing the milling time involved in the process (Ahmad et al., 2020; Liu et al., 2018a; Ma et al., 2022).

Figure 4 – Polarized light microscope images of starch. (a-b) control; (c-n) milled starch: (c-d) 10 h (milling time), 1:6 (mass ratio of starch to balls); (e-f) 20 h, 1:6; (g-h) 30 h, 1:6; (i-j) 10 h, 1:20; (k-l) 20 h, 1:20; (m-n) 30 h, 1:20. The darker images for each pair were taken under polarized light, and the lighter images were not.



Source: Made by the author.

4.3.2. Fourier transform infrared spectroscopy (FTIR)

The distinctive starch bands visible in all the observed infrared spectra include the O–H stretch band at $3500 - 3000 \text{ cm}^{-1}$, the C–H stretch band at 2910 cm^{-1} , and the anhydroglucose stretching vibration band at approximately 950 cm^{-1} , all characteristic of starch. No uncharacteristic band appeared, which indicates that the energy involved in the milling process did not cause the addition or removal of any chemical groups (Goiana et al., 2021; Han et al., 2013; Oliveira et al., 2018). The ratio between the intensity of $995/1044 \text{ cm}^{-1}$ bands was used as an indicator of the ordered structure of the starch (Marenco-Orozco; Rosa; Fernandes, 2022). These ratios are shown in Table 1.

Table 1 – $995/1044 \text{ cm}^{-1}$ band ratio for control and milled starch.

| Sample | $995/1044 \text{ cm}^{-1}$ (%) | Sample | $995/1044 \text{ cm}^{-1}$ (%) |
|-----------------|-----------------------------------|------------------|-----------------------------------|
| Control | 64.9 ± 0.1^d | 1 h (1:20 ratio) | $65.6 \pm 0.6^{c,d}$ |
| 1 h (1:6 ratio) | $65.4 \pm 0.5^{c,d}$ | 5 h (1:20 ratio) | 66.9 ± 0.3^c |

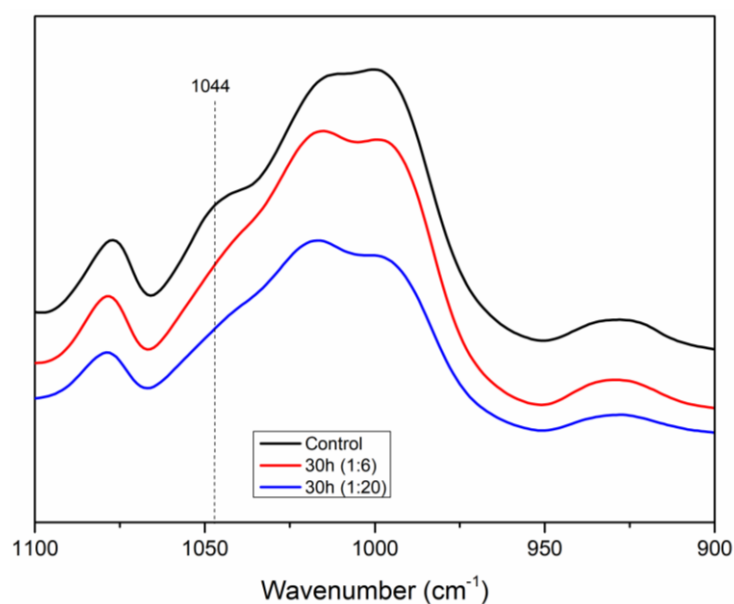
| | | | |
|------------------|-------------------------|-------------------|-------------------------|
| 5 h (1:6 ratio) | 66.4 ± 0.6 ^c | 10 h (1:20 ratio) | 67.9 ± 0.5 ^c |
| 10 h (1:6 ratio) | 66.9 ± 0.2 ^c | 20 h (1:20 ratio) | 70.0 ± 0.9 ^b |
| 20 h (1:6 ratio) | 69.5 ± 0.3 ^b | 30 h (1:20 ratio) | 73.9 ± 1.2 ^a |
| 30 h (1:6 ratio) | 68.9 ± 0.7 ^b | ----- | ----- |

Values not marked by the same letter are significantly different ($\alpha < 0.05$).

Source: Made by the author.

Changes within this range can be utilized as a disturbance sign of the ordered structure of the starch granule because the spectral area between 1050 and 950 cm^{-1} is sensitive to the short-range double helix structural alteration (Van Soest et al., 1995). Since the intensity of the 1044 cm^{-1} band diminishes as the amorphous stage increases, the 995/1044 cm^{-1} ratio grew as milling time increased by a total of 9%, indicating a drop in the starch structure order (Li et al., 2020; Pozo et al., 2018). The most milled granules (20 h and 30 h for both ratios) also showed the highest 995/1044 cm^{-1} ratio, indicating a more amorphous structure than the other samples, corroborating the light microscopy analysis (Figure 4) and the SEM images (Figure 3). Figure 5 shows the apparent drop in the intensity of the 1044 cm^{-1} band of the 30 h milled starch (both ratios) in contrast to the control starch, which indicates the increase in the 995/1044 cm^{-1} ratio and the resulting decrease in the structural order of the starch granules.

Figure 5 – Infrared spectra in the 900 to 1110 cm^{-1} region for the samples of starch milled for 30 h (both ratios) and control starch.

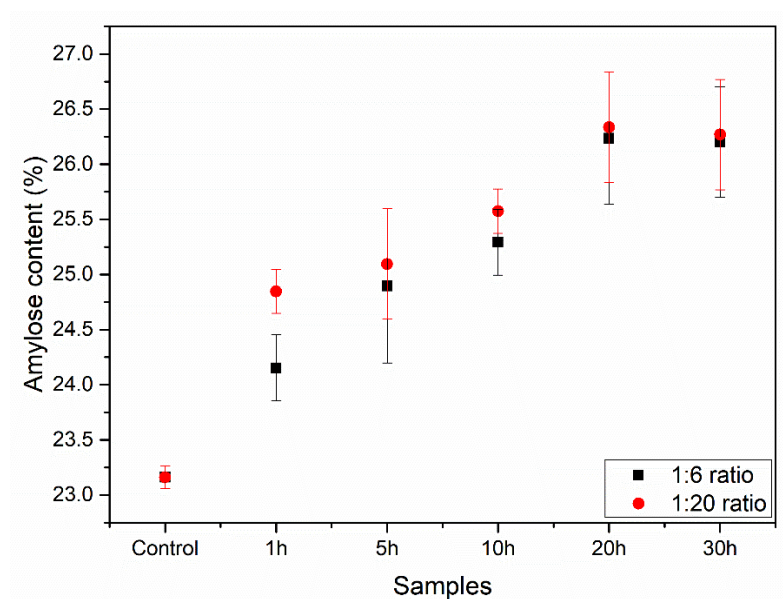


Source: Made by the author.

4.3.3 Amylose content

The amylose content peaked at 20 h of milling for both ratios and then reached a plateau (Figure 6). An increase in milling duration caused this rise in amylose content. Amylopectin, a more rigid and ramified structure, can be partially fractured in the milling process, increasing the percentage of amylose content. This rise in the amylose content may be connected to the fracture of the starch granules caused by the ball mill, as observed in the SEM analysis (Figure 4) (Apriyanto; Compart; Fettke, 2022; Huang et al., 2008). The plateau reached at 20 h may be the result of the high degree of heterogeneity in the starch granule size after milling, which led to the production of numerous granules with varying amylose contents because of different degrees of breakage in each granule, as seen in the SEM images.

Figure 6 – Amylose content (%) for all the starch samples, milled and control.



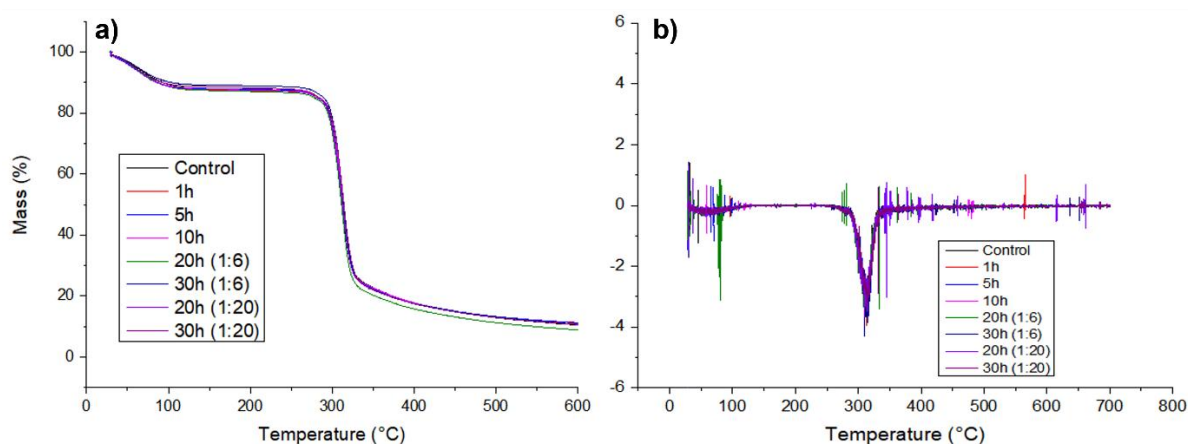
Source: Made by the author.

4.3.4 Thermogravimetric analysis (TGA)

Figure 7 shows all the thermograms of the studied starch samples. The first weight loss event was seen in the TG graphs at approximately 100 °C due to starch hygroscopicity, which is connected to moisture loss from the leftover water associated with the starch molecules. Next, starch degradation was observed at 300 °C, with a Tonset for all samples at approximately 297 °C, showing the breakdown of the anhydroglucose chains, which is consistent with the results for starch in the literature (Apostolidis et al., 2023; Chen et al., 2023; Liu et al., 2009;

Zhang et al., 2022). The ball-milling procedure altered the structure of corn starch, but the thermal profile remained constant at all milling times (1, 5, 10, 20, and 30 h) and ratios (1:6 and 1:20). Therefore, the thermal stability of starch was unaffected by the ball-milling process.

Figure 7 – TG (a) and DTG (b) curves for control and milled starch.

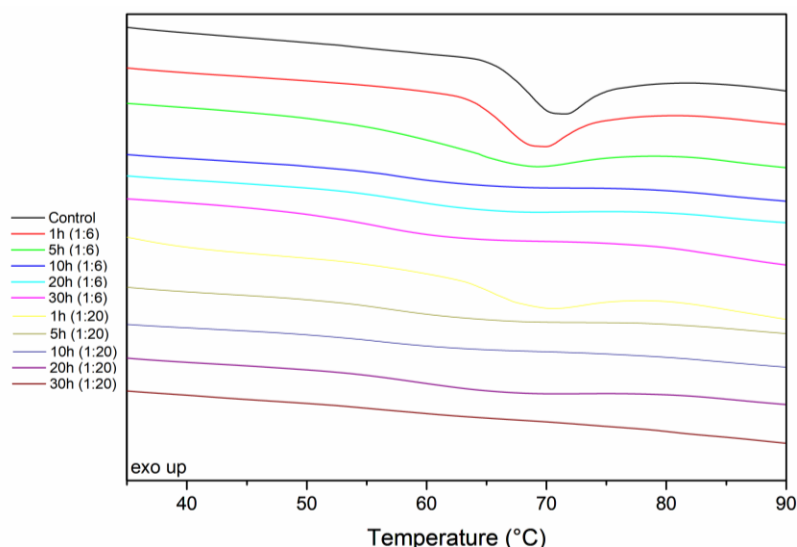


Source: Made by the author.

4.3.5 Differential scanning calorimetry (DSC)

Figure 8 shows the endothermic event that is clearly detected in the control sample and becomes more subtle in the samples as milling time and ratios increase. Starch gelatinization is represented by this endothermic event at approximately 70 °C. As previously stated, ball-milling disturbs the crystalline structure of the starch, which can facilitate the gelatinization process, as evidenced by the DSC results (Oliveira et al., 2018a). As demonstrated, amylopectin degradation occurs in ball-milled starches, promoting the formation of disordered amorphous regions that are easily accessible to water and allowing gelatinization to occur at lower temperatures (Liu; Hong; Zheng, 2017; Singh; Kaur; McCarthy, 2007).

Figure 8 – Differential scanning calorimetry curves for control and milled starch.



Source: Made by the author.

As milling time and ratio rise, there is a more visible change in enthalpy, not only does the gelatinization process begin at a lower temperature but less energy is required to gelatinize the milled starch (Table 2). The peak is essentially nonexistent in the samples milled at a 1:20 ratio for 10, 20 and 30 h showing that the sample gelatinized, at least partially, during the period it was resting in water prior to measurement and thus gelatinized at ambient temperature. These results corroborated with the FTIR, and microscopy results suggests a partial disturbance in the starches crystalline structure which makes the gelatinization process easier, but this crystalline disturbance is not accentuated enough for it to have a direct effect on overall thermal stability and the degradation of the anhydroglucose chains, evidenced by the similar thermal profile obtained in the TGA results (Figure 7) (Liu et al., 2013; Yang et al., 2022).

Table 2 – Gelatinization enthalpy, peak and end temperature of starch samples.

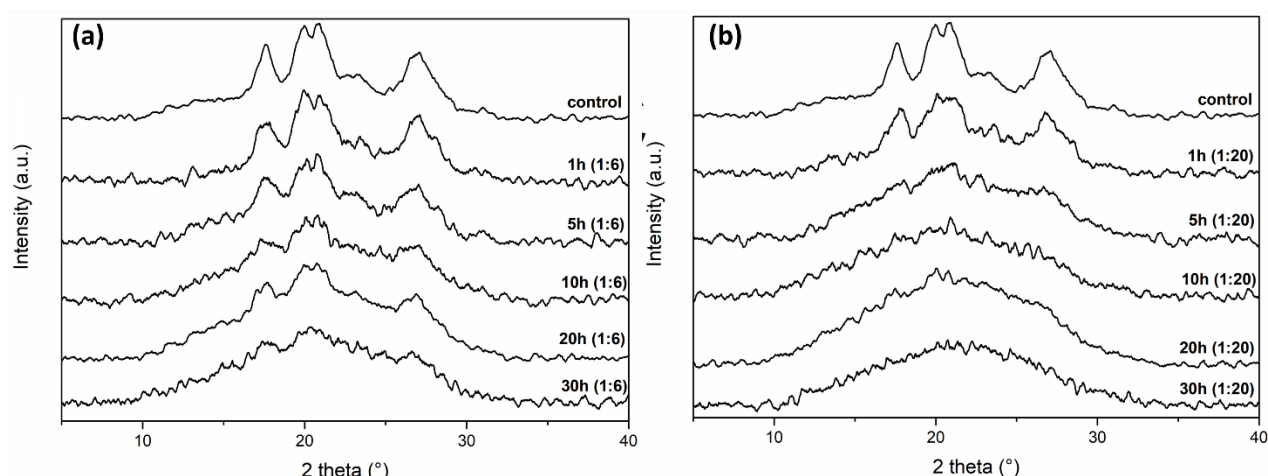
| Sample | ΔH_{gel} (J.g ⁻¹) | Peak Temperature (° C) | End Temperature (° C) |
|-------------------|--|------------------------|-----------------------|
| Control | 1.86 ± 0.21^a | 71.4 | 83.5 |
| 1 h (1:6 ratio) | 1.75 ± 0.15^a | 69.6 | 82.4 |
| 5 h (1:6 ratio) | 1.48 ± 0.11^b | 69.2 | 79.4 |
| 10 h (1:6 ratio) | 0.76 ± 0.10^d | 64.9 | 77.7 |
| 20 h (1:6 ratio) | $0.72 \pm 0.09^{d,e}$ | 65.7 | 77.6 |
| 30 h (1:6 ratio) | 0.64 ± 0.07^e | 61.8 | 74.6 |
| 1 h (1:20 ratio) | 0.88 ± 0.05^c | 69.9 | 81.2 |
| 5 h (1:20 ratio) | 0.84 ± 0.09^c | 65.3 | 77.3 |
| 10 h (1:20 ratio) | 0.38 ± 0.06^f | 62.3 | 75.1 |
| 20 h (1:20 ratio) | 0.24 ± 0.08^f | 61.9 | 74.3 |

| | | | |
|-------------------|-------------------|------|------|
| 30 h (1:20 ratio) | 0.01 ± 0.00^g | 61.5 | 66.7 |
|-------------------|-------------------|------|------|

Values not marked by the same letter are significantly different ($\alpha < 0.05$).
Source: Made by the author.

4.3.6 X-ray diffraction (XRD)

Figure 9 – Diffractograms of the 1:6 (a) and 1:20 ratio (b) milled starch samples and the control sample.



Source: Made by the author.

The diffractograms of the examined samples are shown in Figure 9, which reveals the expected A-type crystal structures typical of corn starch. A doublet around $19 - 20^\circ$ and significant crystalline peaks at about 17° and 27° can be seen in the diffractograms. Minor variations in peak degrees are seen, which are caused by the analysis using Co tubes rather than Cu tubes (Rodriguez-Garcia et al., 2021; Silva et al., 2019).

For both ball/mass ratios, the crystalline peaks showed reduced intensity as milling time increased, indicating a decline in structural organization and resulting in a lower crystalline index (CrI), as shown in Table 3. For shorter milling periods, the higher ball/mass ratio had a more significant impact on the CrI, as shown by a visible disturbance in the peaks and consequently lower CrI values (Pozo et al., 2018). The decrease in CrI supports the polarized microscopy results (Figure 4), which demonstrate that the milling procedure successfully decreased the crystallinity of the starch samples.

Table 3 – Crystalline indexes (CrI) of the control and milled starch samples.

| Sample | CrI (%) | Sample | CrI (%) |
|-----------------|---------|------------------|---------|
| Control | 34.8 | 1 h (1:20 ratio) | 28.6 |
| 1 h (1:6 ratio) | 31.9 | 5 h (1:20 ratio) | 12.9 |

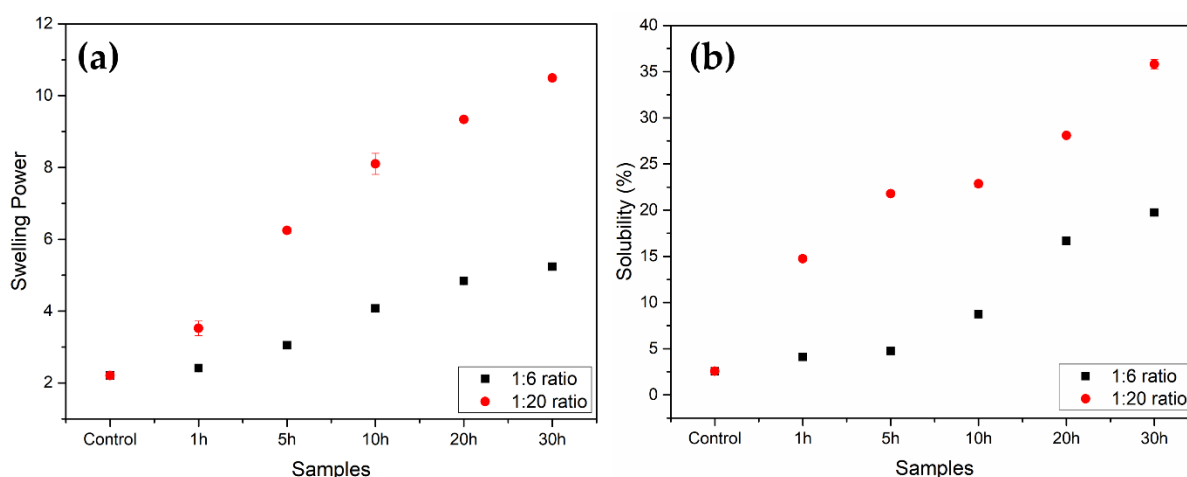
| | | | |
|------------------|------|-------------------|-------|
| 5 h (1:6 ratio) | 27.0 | 10 h (1:20 ratio) | 8.3 |
| 10 h (1:6 ratio) | 15.9 | 20 h (1:20 ratio) | 2.8 |
| 20 h (1:6 ratio) | 10.7 | 30 h (1:20 ratio) | 2.7 |
| 30 h (1:6 ratio) | 8.4 | ----- | ----- |

Source: Made by the author.

4.3.7 Swelling power (SP) and Solubility (S%)

Figure 10 shows that as the ball-milling time and ratio rose, the swelling power (SP) and solubility (S%) of the samples increased. The ball-milling procedure gradually enhanced the capacity of the starch granules to retain water in their structure. A significant difference is evident between the 1:6 ratio and 1:20 ratio samples due to the increased fragmentation of the structures, as observed by the SEM images (Figure 3).

Figure 10 – Swelling power (a) and Solubility (b) of the native corn starch sample (Control) and the ball-milled starch samples.



Source: Made by the author.

The starch crystalline structure is broken when it is heated in excess water due to the breakdown of intramolecular and intermolecular hydrogen bonds. Water molecules then establish hydrogen bonds with the exposed hydroxyl groups of amylose and amylopectin, causing granule swelling to rise. The amount of interaction between starch chains within the amorphous and crystalline domains has a major impact on swelling power (Fu et al., 2012; Waterschoot; Gomand; Delcour, 2016). Moreover, the complete or partial breakage of the starch crystalline structure via ball milling proved to have a similar effect to temperature on the SP and S% results. The granules become more fragmented as both the time and ratio of ball

milling increase (Figure 3), making the structure more accessible to water. This can be correlated with the partial destruction of the amylopectin chains and changes in the amylose content since both properties are associated with the swelling power capacity and solubility of the starch. The water, even at room temperature, can easily permeate the granule (in the more milled samples), causing the swelling power and solubility to rise significantly from the native starch (control) to, especially, the 1:20 ratio samples. This shows SP and S% values compatible with those of gelatinized starch mentioned in other studies (Abegunde et al., 2013; Fu et al., 2012; Mandala; Bayas, 2004; Waterschoot; Gomand; Delcour, 2016).

4.3.8 *Rheology*

Table 4 lists all the rheological data acquired for the starch samples, both control and milled at various times and ratios. The gelatinization temperature of the starch (TGel) decreased continuously as both time and ratio increased, resulting in a pregelatinized starch generated purely through milling. The gelatinization of the 20 and 30 h samples (1:20 ratio) was not captured by the equipment because the samples were gelatinized simply by mixing with water as a preparation for the analysis at room temperature (25 °C), as deduced from the DSC analysis (topic 4.3.6).

During temperature and frequency sweep testing of starch suspensions, the dynamic rheometer enables continuous assessment of dynamic moduli and viscosity. The storage modulus (G') is a measure of the energy stored and recovered from the material every cycle, whereas the loss modulus (G'') is a measure of the energy dissipated or lost per cycle of sinusoidal deformation (Narpinder et al., 2003). When compared to the control sample, the viscosity, G' , and G'' increased at the beginning of the milling process (1, 5, and 10 h ratio 1:6), indicating that partial fragmentation of the starch via ball milling facilitates the gelatinization process, forming a more viscous gel after sample preparation (90 °C for 10 min). However, as milling time increases, the viscosity, G' and G'' begin to decrease, indicating that while initial fragmentation causes the starch to form a more viscous gel, as the starch is further fragmented, this gel begins to lose viscosity, reaching a minimum in the 30 h 1:20 ratio sample. This drop in viscosity, as well as G' and G'' , is because the amylopectin chain decreases as the granule is broken, so the gel generated by this starch is less viscous than those made by less milled samples (Ahmad et al., 2020; Chen et al., 2023; Desam et al., 2021).

Thixotropy is a property associated with starch gel and paste rheoinstability. Simply put, thixotropy measures how well or poorly a gel or paste may return to its initial conformation

after being subjected to a shear rate fluctuation. The greater the thixotropy, the greater the gap between the initial and end states and the higher the rheoinstability of the gel or paste. The thixotropy of the samples decreased as the milling time and ratio increased, reaching low numbers (< 2.2) for the 10, 20, and 30 h (1:20 ratio) samples. This behavior occurs because the more milled samples have smaller granules, and their structure is formed by weaker bonds that can be easily restored once the sheer rate decreases, whereas the less milled and control samples have larger granules and thus more complex bonds that would take more time to completely restore, if ever (Ma; Zhu; Wang, 2019; Sikora et al., 2015; Yang et al., 2022).

Table 4 – Rheological parameters of the control and milled starch samples.

| Samples | TGel (°C) | Viscosity (η) [cP] | Storage module (G') [Pa] | Loss module (G'') [Pa] | Thixotropy |
|-------------------|--------------|------------------------------|-----------------------------|---------------------------|------------|
| Control | 69.1 | 889.7 | 2.24 | 5.12 | 27.02 |
| 1 h (1:6 ratio) | 63.4 | 1601.00 | 3.33 | 9.49 | 23.77 |
| 5 h (1:6 ratio) | 61.3 | 921.20 | 1.32 | 5.64 | 17.38 |
| 10 h (1:6 ratio) | 55.9 | 969.90 | 1.28 | 5.96 | 9.89 |
| 20 h (1:6 ratio) | 51.6 | 255.90 | 0.28 | 1.58 | 9.15 |
| 30 h (1:6 ratio) | 50.1 | 119.20 | 0.12 | 0.74 | 4.75 |
| 1 h (1:20 ratio) | 62.7 | 660.70 | 1.24 | 3.97 | 16.74 |
| 5 h (1:20 ratio) | 60.1 | 352.90 | 0.76 | 2.09 | 11.14 |
| 10 h (1:20 ratio) | 51.4 | 173.20 | 0.35 | 1.03 | 2.04 |
| 20 h (1:20 ratio) | * | 148.60 | 0.23 | 0.91 | 2.16 |
| 30 h (1:20 ratio) | * | 81.62 | 0.15 | 0.49 | -0.07 |

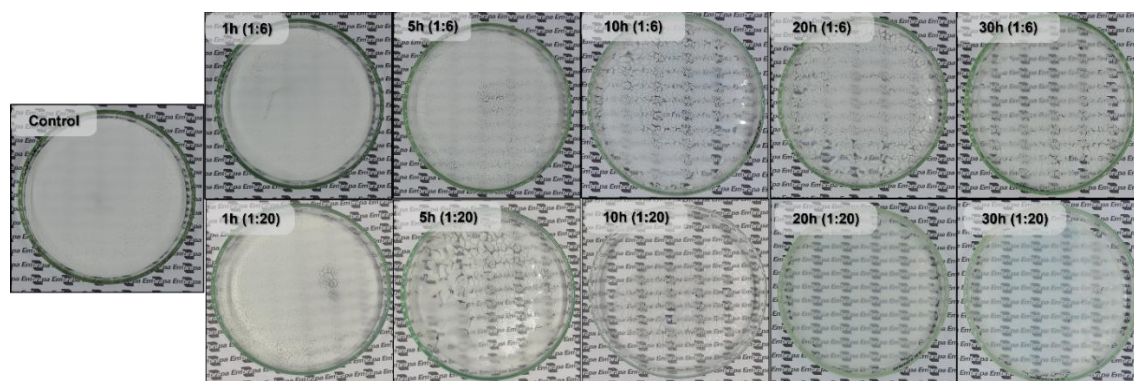
* Samples gelatinized at room temperature during sample preparation

Source: Made by the author.

4.3.9 Film forming ability

Figure 11 shows films formed by all starch samples and evidence of how the milling time affected the starch ability to gelatinize at room temperature (30 °C) and create films. The control starch suspension, once dried, and forms a thin opaque layer of starch powder. However, as the milling time increased, the starch suspensions dried and formed more uniform and transparent films. The 10, 20 and 30 h milled samples at a 1:20 ratio produced the best-looking films, but the 20 h (1:20 ratio) is the one that showed a completely homogenous and see-through film with the shortest milling time possible, with 10 h (1:20 ratio) being a close second, since its film has some parts where the starch was not completely gelatinized. To the best of the authors' knowledge, no work has described, in depth, the impact of milling on the gelatinization of starch, despite the impressive discoveries reported in the literature about starch milling.

Figure 11 – Films formed by oven drying starch suspensions (10%) at room temperature (30 °C) using control and milled starches.



Source: Made by the author.

According to Goiana et al. and Oliveira et al. (Goiana et al., 2021; Oliveira et al., 2018a), most studies that use starch films heat the starch and water to approximately 90 °C for starch gelatinization before adding a plasticizing agent, such as glycerol, to ensure film resilience. However, milled starches with a lower gelatinization temperature were able to form a thin and fragile film without heating or the addition of any plasticizing agents.

A more fractured granule has a larger surface area and is more susceptible to the effects of water. Water can enter the grain quickly, swelling it and causing gelatinization of the starch. This behavior displayed by the milled starch is related to the fracture caused by the milling process. Therefore, milling is an efficient way to reduce the starch gelatinization temperature (Chakraborty et al., 2022; Torres; De-la-Torre, 2022; Wang et al., 2022).

4.4 Conclusions

Ball-milling altered the starch granule physical makeup by shattering it. These fractures made it easier for water to access the granule, boosting the granule's reactivity and decreasing its gelatinization temperature. The 10 h milled starch at a 1:20 starch/ball mass ratio underwent enough physical and gelatinization temperature changes, with the shortest milling time possible, to be used as a thickening agent in thermally sensitive applications, such as the pharmaceutical industry and some food products. However, samples milled at different times can have different applications, such as the 1 h milled starch at a 1:6 mass ratio forming a more viscous gel than the control starch, making it a more efficient thickening agent than the non-milled starch. In

addition, this research made a discovery: a process as simple as milling starch can drastically change the gelatinization temperature of starch leading to effects on its rheological properties.

5 OPTIMIZING PICKERING EMULSION STABILITY: UNVEILING THE SYNERGISTIC POTENTIAL OF STARCH NANOPARTICLES AND CHITIN NANOCRYSTALS.

Abstract

We demonstrate enhanced Pickering stabilization of chemically modified starch nanoparticles (SNP) through their combination with chitin nanocrystals (ChNC), which also impart antimicrobial properties. The stabilization achieved with a 1:1 (SNP:ChNC) ratio surpasses that of the individual components, exhibiting a synergistic effect compared to neat SNP and the 10:1 and 5:1 systems. Emulsion stability was further improved by applying thermal pre-treatment to the aqueous phase before homogenization. The heat-treated 1:1 emulsion maintained a consistent droplet size ($\sim 3.4 \mu\text{m}$) over three months, even after slow creaming. This stability is attributed to SNP adsorption at the oil-water interface, providing interfacial protection, while ChNC forms a colloidal network in the continuous phase, preventing Ostwald ripening and coalescence.

Keywords: Chitin nanocrystals; Starch nanoparticles; Gelatinization.

5.1 Introduction

Emulsions, consisting of a liquid continuous phase with dispersed droplets, are inherently thermodynamically unstable. To achieve kinetic stability, emulsions benefit from physicochemical and rheological effects. Typically, stability is enhanced by the adsorption of surfactants at the droplet interface (Guida; Aguiar; Cunha, 2021; Kalashnikova et al., 2013; Lu; Tian, 2021a). Common examples of emulsions include mayonnaise, milk, butter, creams, and moisturizers, among others (David Julian McClements, 2015; Lv et al., 2021).

However, traditional petrochemical surfactants present challenges such as toxicity, foam formation, and interactions with biological systems. Pickering emulsions offer a promising alternative to address these issues. Unlike conventional emulsions, Pickering emulsions are stabilized by solid particles that adsorb at the colloidal interface, providing steric hindrance to coalescence. During homogenization, these particles adsorb to droplet surfaces, acting as

physical barriers that prevent coalescence and enhance kinetic stability (Cui et al., 2021b; Hadi et al., 2020; Keramat; Kheynoor; Golmakani, 2022; Zhu et al., 2021).

Effective Pickering emulsion stabilization requires particles with balanced wettability. Biobased alternatives such as starch have gained increasing interest due to their sustainability and functionality (Bai et al., 2021). Starch, a common plant-derived polysaccharide, has a unique semicrystalline structure composed of amylose and amylopectin. Both are glucose polymers linked by glycosidic bonds, yet they differ significantly in structure, properties, and functionality (Leal-Lazareno et al., 2025). Amylose is primarily linear, with glucose units joined by α -1,4 glycosidic bonds and occasional α -1,6 linkages, allowing it to adopt a helical conformation in aqueous solutions stabilized by hydrogen bonding. In contrast, amylopectin is highly branched, with glucose units linked by α -1,4 bonds in linear regions and α -1,6 bonds at branching points. This branching increases its water solubility and molecular weight. While amylose forms firm gels upon cooling, amylopectin imparts a softer, more viscous texture (De Dios-Avila et al., 2024; Zhang et al., 2024).

Due to their high surface area and biocompatibility, starch nanoparticles (SNPs) have been explored for film-forming applications and Pickering emulsion stabilization. Smaller starch particles typically provide greater interfacial coverage and improved emulsion stability due to their higher specific surface area (Lv et al., 2021; Marto et al., 2019; Xu et al., 2023). Hydrolysis is a widely used method for SNP production, but physical approaches such as ball-milling are emerging as environmentally favorable alternatives. Ball-milling disrupts the crystalline structure of starch granules, reducing particle size and significantly lowering the temperature —sometimes to ambient levels— of gelatinization, a process that disrupts the double-helix structure of amylose in starch, enhancing its flexibility and dispersibility. This mechanical treatment also decreases starch hydrophilicity, making ball-milling a promising, sustainable technique for SNP production over traditional chemical processes (Bangar et al., 2023; Barros et al., 2023; Limpongsa; Soe; Jaipakdee, 2021; Oliveira et al., 2018b; Xu et al., 2020).

To improve the interfacial properties of starch particles, they are often esterified with 2-octen-1-ylsuccinic anhydride (OSA), introducing hydrophobic alkyl chains that render the particles amphiphilic. While OSA modification is FDA-approved and considered safe for food applications, its disposal and handling are more challenging compared to acid- or base-treated alternatives (Wang et al., 2022; Xu et al., 2023; Zhu, 2019).

An optional approach to chemical modification is the combination of biobased particles, leveraging their individual properties to enhance Pickering emulsion stability. Here, we propose a synergistic system combining ball-milled SNPs and chitin nanocrystals (ChNCs) to stabilize emulsions. ChNC complement the partial hydrophobicity imparted to SNPs during milling, enhancing their adsorption at the oil-water interface. Additionally, ChNCs provide electrostatic stabilization and act as a physical barrier against droplet coalescence by promoting repulsive interactions. Thermal treatment of starch may further reinforce the interactions between SNPs and ChNCs, improving overall stability (Lv et al., 2021; Xu et al., 2020, 2023).

During gelatinization, starch loses its structural integrity, leading to the self-assembly of SNPs into smaller spheres, which allows for denser packing at the oil-water interface. This structural rearrangement contributes to improved emulsion stability. Additionally, the presence of free gelatinized starch in the aqueous phase increases viscosity, offering an additional mechanism for stabilization. Overall, gelatinization plays a crucial role in modifying starch properties to enhance the stability and performance of colloidal systems (Liu et al., 2018; Xu et al., 2020).

In this study, we investigate the synergistic effects of ChNCs and SNPs as interfacial stabilizers, avoiding chemical modifications while maintaining high-performance stabilization. Our goal is to develop a safe, high-quality formulation suitable for food applications.

5.2 Materials and Method

5.2.1 *Materials*

Commercially available corn starch (Kimimo), sunflower seed oil (Mazola), Nile red dye (Sigma-Aldrich), Nile blue (Sigma-Aldrich), fluorescein 5(6)-isothiocyanate (FITC) (Sigma-Aldrich), hydrochloric acid 37% (Sigma-Aldrich) and glacial acetic acid (Sigma-Aldrich) were all used as received.

Commercial corn starch has an approximate molecular weight of 2×10^7 g/mol, which varies with the amylose-to-amylopectin ratio; higher amylopectin increases molecular weight. The starch used in this study contained 23.16% amylose (Barros et al., 2023).

The starch nanoparticles (SNP) were obtained through ball-milling following our previously published method (Barros et al., 2023). The starch was milled for 20 h using a

ceramic system (20 cm diameter) equipped with ceramic balls (1.5 cm) and operated at a starch/ball mass ratio of 1:20 at 25 °C

The chitin nanocrystals (ChNC) were obtained following the method proposed by (Larbi et al., 2018) and obtained from chitin extracted from crab shells (*Metacarcinus magister*) according to our previous work, (Su et al., 2024). Briefly, 1 g (dry weight) of ChNC was added to 30 mL HCl 3M solution and heated for two hours at 90 °C. The reaction was stopped by dilution with 800 mL of cold milli-Q water. After centrifuging the ChNC suspension for 15 min at 10,000 rpm and discarding the supernatant, the particles were dialyzed to pH 4. The ChNC suspension (pH 4) was sonicated at 40% intensity for 15 min (5 s on and 2 s off). Finally, the pH was adjusted to 3 with acetic acid and the suspension was stored until use. The deacetylation degree of the ChNC was measured to be 22%.

5.2.2 Preparation of the Pickering emulsions

The aqueous phase of the emulsions (1% wt total solids) was prepared using different SNP:ChNC ratios (10:1, 5:1, and 1:1) and two neat (reference) aqueous phases were prepared using SNP or ChNC. All aqueous phases were adjusted to pH 3 using acetic acid before addition of the oil phase.

To create a 10:90 Pickering emulsion, 10% wt sunflower oil was added to the aqueous phase. The mixture was immediately emulsified using a high shear force mixer (IKA® Ultra – Turrax T25 easy clean, Breisgau, Germany) at 12000 rpm for 1 min. Following homogenization, the emulsions underwent four rounds of 2-min (30 s intervals) sonication (60% potency) in an ice bath to prevent heating of the sample (Sonifier 550, Branson, Connecticut, USA). The emulsions were vortexed for 30 s in between each sonication.

Emulsions both with and without heating treatment of the aqueous phase were studied. For the heat treated (HT) emulsions the starch suspension was heated to 60 °C for 10 min to ensure gelatinization of the starch particles before the addition of ChNC, when present, and oil. The non-pre gelatinized emulsions are referred to as control in this work. In our study, the gelatinization process occurred at room temperature in contrast to typical native starch gelatinization which is carried out at 80 °C. The heat treatment (60 °C), previously mentioned, was applied to ensure that all the particles present in the samples were fully gelatinized (Barros et al., 2023).

5.2.3 Kinetic stability of emulsions

Emulsion phase separation was evaluated at 21 °C, over five months. The volume of separated phases was measured using GIMP (version 2.10.36) and the Separation index (SI) was calculated according to equation Eq. (1)

$$\text{Separation index [\%]} = \left(\frac{H_S}{H_T} \right) \cdot 100 \quad (1)$$

where H_T is the total height of the emulsion column and H_S is the height of the serum bottom phase.

A LUMiSizer® (LUM GmbH, Berlin, Germany) dispersion analyzer was used to determine the creaming velocity and instability index of the emulsion samples and the sedimentation velocity of the aqueous phases. About 430 µL of the sample was placed within the low-volume polypropylene LUMiSizer cuvette. The analysis consisted of 300 10 s runs at 4000 rpm and 25 °C, using an 870 nm wavelength.

5.2.4 Emulsion morphology

An Eclipse LV100N POL (Nikon, Tokyo, Japan) optical microscope equipped with a camera attachment was used to capture the images of the emulsion droplets as soon as they were prepared. To view the droplets under a bright field, 50 µL of the emulsion sample was placed in a glass slide with a glass cover.

The dyed emulsion was examined using Confocal Laser Scanning Microscopy (Olympus FV1000, Tokyo, Japan) to see how the starch and chitin particles were organized in the system, right after being prepared. Nile Blue (Sigma-Aldrich) was used to dye the SNP, and FITC was used to dye the chitin nanocrystals, in accordance with Lopes et al. (2019) with some adjustments. 100 mL of dehydrated ethanol and 50 mL of FITC solution (0.5 mg FITC/1 mL ethanol) were combined with 40 mL of 1% wt ChNC suspension (pH 3). The combination was then stirred for three hours in the dark. Following a pH adjustment with NaOH (0.1 M) to 7.0, the solution was centrifuged for 3 min at 5000 rpm, and the precipitate was repeatedly washed with milli-Q water until the dye was no longer visible in the supernatant. The labeled ChNC was freeze-dried and used to emulsion preparation according to section 5.2.3.

5.2.5 Droplet size and Electrostatic charges

A Mastersizer® 3000 (Malvern, Worcestershire, United Kingdom) was used to determine the emulsions' droplet size distribution. The measurements were performed with the assumption that the droplets were completely spherical. The results were referred to as surface area mean diameter, also known as Sauter mean ($D_{[3,2]}$). These measurements were carried out as soon as the emulsions were produced and every 30 days over a 5-month period.

A Zetasizer® nano series Nano-ZS (Malvern, Worcestershire, United Kingdom) was used to evaluate the zeta potential (ZP) of samples. To perform the measurements, the emulsions were diluted using milli-Q water 1:100 with pH 3 acetic acid solution at 21 °C. Additionally, the ZP of the aqueous phases alone was determined.

The SNP and ChNC particles were observed under TEM imaging to better understand their morphology and size when in a water suspension. The H7600 TEM (Hitachi, Tokyo, Japan) was used to obtain these images with an acceleration voltage of 120 kV.

5.2.6 Stability analysis (pH and temperature)

For the pH stability analysis, 0.5 mL of the HT emulsions were added to 1 mL of a solution with a known pH (3, 5, and 7), with the pH of these solutions being adjusted using HCl. The droplet size and separation index were evaluated immediately after the dilution was prepared and again after 7 days.

For the temperature stability analysis, the emulsions were transferred to 2 mL vials and stored at a constant temperature (4 °C and 21 °C) for 7 days. The droplet size and creaming index were measured immediately after the emulsions were prepared and once more after 7 days of storage at constant temperatures.

5.2.7 Rheological properties

The viscosity of the emulsion samples as well as just the aqueous phases were recorded with the help of an Anton Paar Modular Compact Rheometer (MCR 302) coupled with a 50 mm diameter plate-plate geometry (PP50) with a 1 mm gap. Flow curve measurements were performed in three steps to avoid thixotropic effects. First a shear rate ramp from 0.1 to 300 s⁻¹ was executed, then the shear rate was brought back to 0.1 s⁻¹ and finally up to 300 s⁻¹ again. All the steps were performed at 25 °C and the last ramp was fitted to the power law equation (Eq. 2) by the least square regression.

$$\sigma = k \cdot \dot{\gamma}^n \quad (2)$$

where σ is the shear stress (Pa), $\dot{\gamma}$ is the shear rate (s^{-1}), k is the consistency index (Pa.s) and n is the behavior index (dimensionless).

The apparent viscosity (η_{ap}) of the samples was determined at 100 s^{-1} following Eq. 3:

$$\eta_{ap} = k \cdot \dot{\gamma}^{n-1} \quad (3)$$

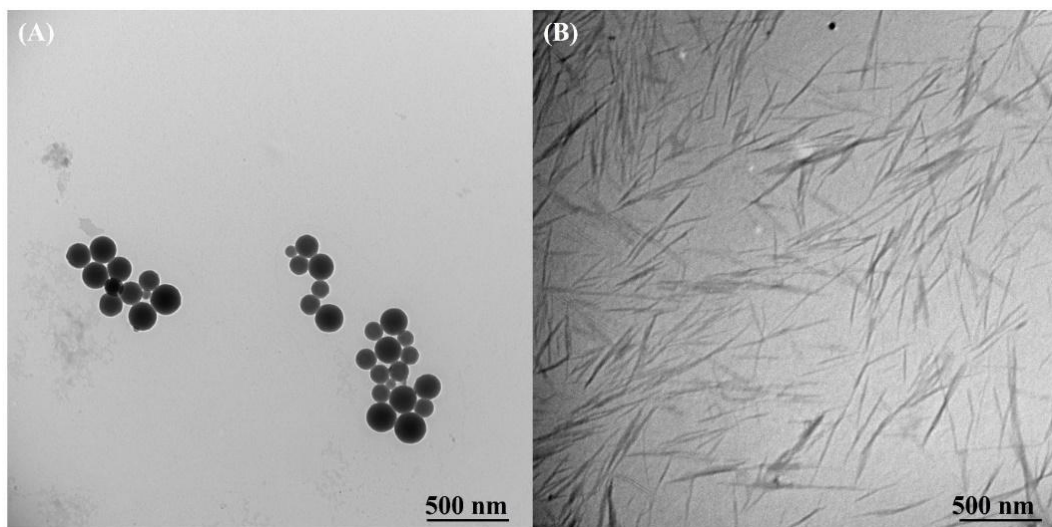
5.3 Results and Discussion

5.3.1 SNP and ChNC morphology and size

Figure 12 shows the TEM images of the SNP and ChNC particles. The SNP particles displayed a size of $119 \pm 32 \text{ nm}$. As also observed by Liu et al. (2019) and Xu et al. (2020), the gelatinized starch tends to self-assemble in spherical shapes (Figure 1A). However, a key difference with previous work is the fact that SNP did not undergo thermal treatment but gelatinized at room temperature (Barros et al., 2023).

The ChNCs have a length of $252 \pm 50 \text{ nm}$ and a width of $22 \pm 4 \text{ nm}$ (aspect ratio of 12 ± 3) (Larbi et al., 2018; Su et al., 2024). The small size of the particles endows high specific surface area and structuring that contributes to the stabilization of the oil-water interface in colloidal systems (Chevalier; Bolzinger, 2013; Lu; Tian, 2021b; Zhu, 2019).

Figure 12 – Transmission electron microscopy (TEM) images of the starch nanoparticles (A) and chitin nanocrystals (B) under 30000x magnification.



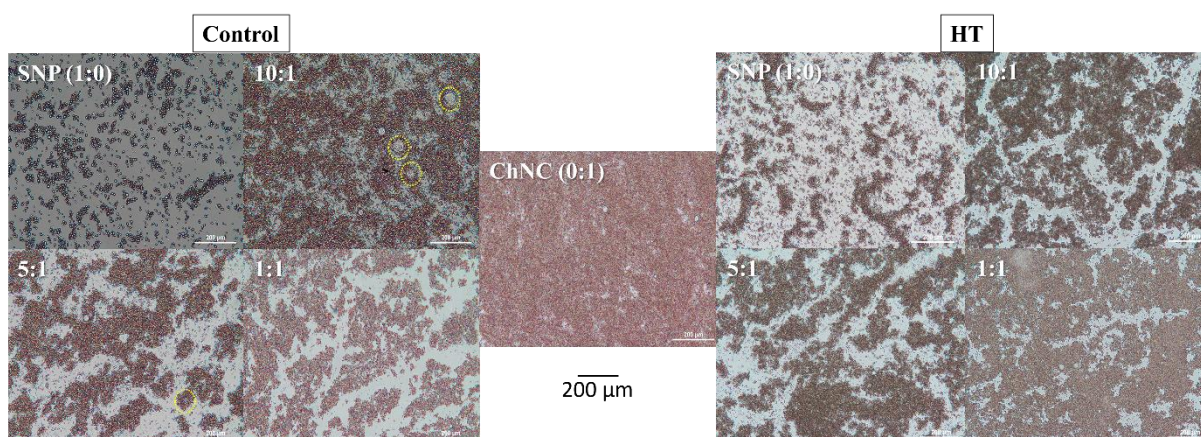
Source: Made by the author.

5.3.2 Emulsion droplet morphology

Both “Control” and “HT” treatments were considered, namely, emulsions in which the aqueous phase did not go through heating and emulsions that used heat-treated aqueous phase, respectively.

The optical microscopy for ChNC-only emulsion, HT, and control emulsions are displayed in Figure 13. The purpose of the 4000x magnification used in this investigation was to display the larger droplet network across the emulsion. It was possible to see nearly whole starch granules in the control samples' microscopy, particularly in the 10:1 and 5:1 samples. In a previously published study, we observed that the starch is broken up by ball milling, leaving a polydisperse particle size, which can account for the presence of these large starch granules (Barros et al., 2023).

Figure 13 – Microscopy of the different SNP:ChNC ratio emulsions, both control and HT, taken at day 0 with 4000x magnification.

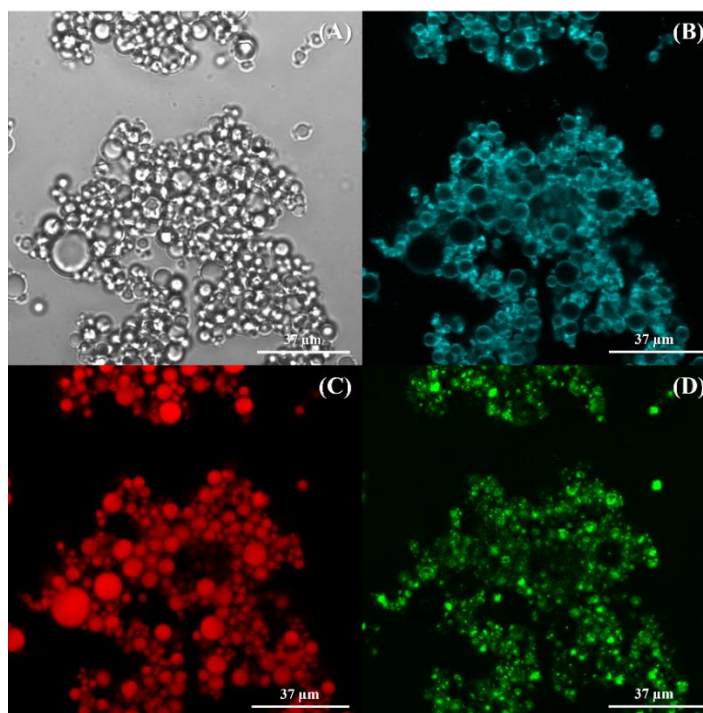


Source: Made by the author.

However, the heat treatment of starch, as previously mentioned, results in smaller and more flexible starch particles that tend to self-assemble into spherical shapes. This process addresses the issue of large starch granules and enhances stability. Consequently, no large starch granules were observed in the images of the heat-treated (HT) samples. The samples with an intermediate concentration of chitin nanocrystals (ChNC) exhibited increased flocculation, which can be attributed to their lower zeta potential and droplet aggregation (Liu et al., 2018; Xu et al., 2020).

The confocal microscopy (CLSM) was used to better understand the disposition of the particles in the sample that had the most promising stability results among the emulsions made with SNP and ChNC, the 1:1 HT sample (Figure 14).

Figure 14 – Confocal Laser Scanning Microscopy (CLSM) images of the 1:1 HT sample, a couple hours after preparation. (A) Bright field image of the emulsion. (B) SNP particles stained with Nile Blue. (C) Sunflower oil droplets stained red. (D) ChNC stained with FITC.



Source: Made by the author.

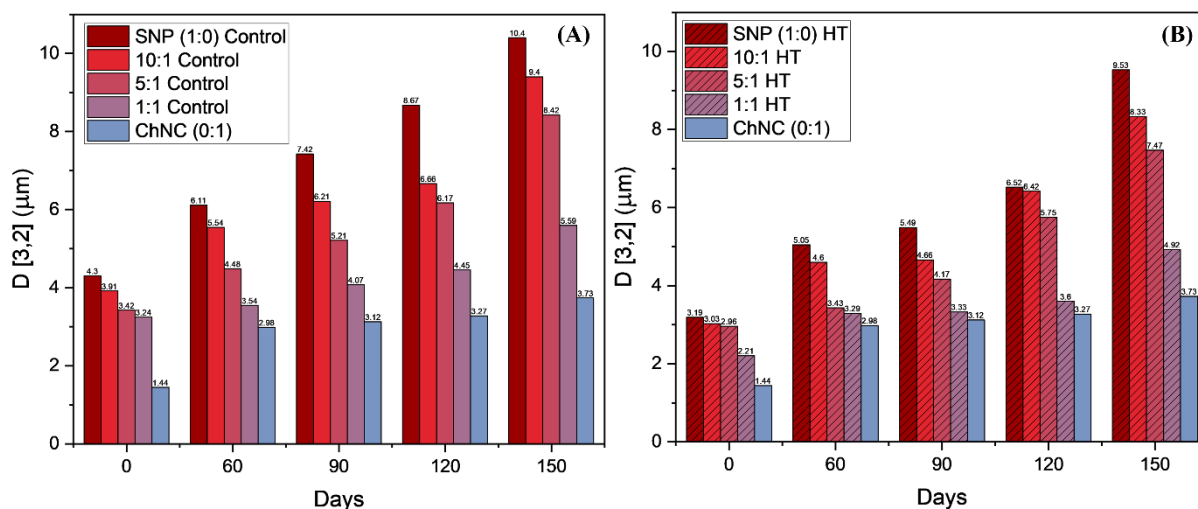
On Figure 14 we can see that the SNP and the ChNC act in two different regions of the emulsions. The SNP (blue) are more present in the interface of the oil droplet (red) granting the emulsion a physical barrier against coalescence on an interface level (Figure 14B), the ChNC (green) is more present in the space between droplets, forming a network of whiskers, acting as a structural barrier between the droplets adding to the overall stability of the system via lowering the mobility of the droplets which in turn leads to less coalescence as well (Figure 14D). Both biopolymers used act in the stabilization of the emulsions but through two completely different stabilization mechanisms, which further supports the hypothesis that both these polymers have a synergistic relationship when used combined in Pickering emulsions stabilization (Ben Cheikh et al., 2021; Su et al., 2024).

Overall, the emulsions with ChNC added have a more compacted droplet disposition. The 1:1 HT sample's densely packed droplet disposition can be attributed to ChNC's propensity to form bridges between the oil droplets, adding an additional layer of steric stability to the system, as seen in Figure 14 (Ben Cheikh et al., 2021; Lee; Chan; Mohraz, 2012).

5.3.3 Droplet size measurements

The emulsions studied had droplet sizes (droplet volume-area diameter – $D_{3,2}$) ranging from 1.4 μm to 4.3 μm on the day of preparation (Figure 4). The droplet sizes observed fall within the expected range for Pickering emulsions and are on the smaller side compared to other studies, which report droplet sizes as large as 40 μm for Pickering emulsions stabilized by starch nanocrystals (Ko; Kim, 2021; Lv et al., 2021).

Figure 15 – Droplet size based on area of droplets for the different SNP:ChNC ratio emulsions for 150 days storage at 21°C, for control (A) and HT (B) samples.



Source: Made by the author.

For the HT samples, droplet sizes were smaller than for the control on all days, as seen in Figure 15, with emphasis on the 1:1 HT sample, which showed results comparable to the ChNC-only sample and showed great stability over time (topic 5.3.5). The heat treated SNP tends to self-assemble into micelles and attach to the droplet surface (Liu et al., 2019). These micelles are more flexible and smaller than the initial SNP which can lead to the better coverage of smaller droplets of oil. This behavior is responsible for the smaller droplet sizes on the HT

samples, an example of this behavior can be observed in Figure 12A. This paired with the inter-droplet stability provided by the ChNC grants the emulsion good overtime stability (Xu et al., 2020).

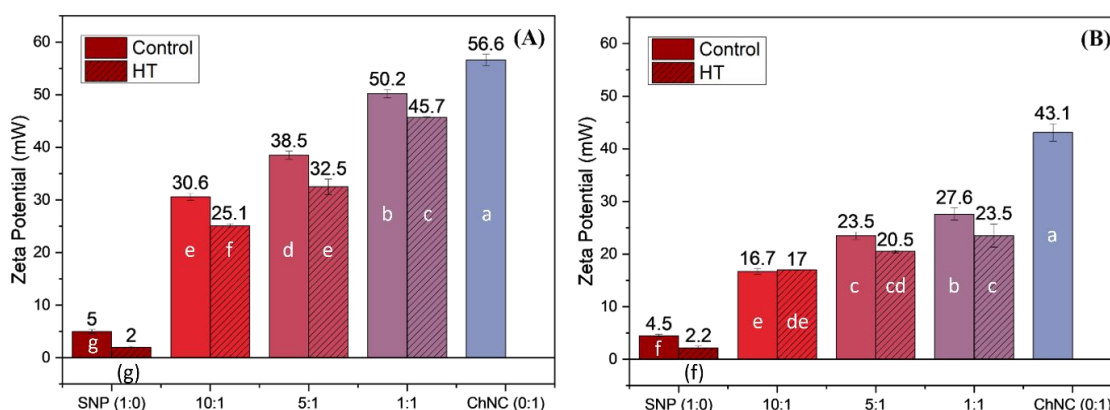
There is a clear and well-known relationship between increased stability and smaller droplets. Coalescence is responsible for the gradual increase in droplet size in emulsions over time. An instability process in the system is triggered when these larger, merging droplets rise to the top of the emulsion due to their increased buoyancy (Bai et al., 2021; Cui et al., 2021b; Lu; Tian, 2021a).

As anticipated, all samples' droplet sizes increased following the 150 days of room temperature storage (Figure 15), leading to the creaming (Figure 17). However, none of the sample emulsions experienced formation of a pure oil phase before 90 days of storage despite the increased droplet size. Again, the 1:1 HT sample deserves special attention since, after 150 days of storage, its droplet size increased by 122%, a much lesser rise than that of the ChNC-only emulsion, which exhibited a 159% increase. The emulsion's droplet size remained within the range of typical Pickering emulsions even after 150 days of storage.

5.3.4 Zeta potential

Figure 16 illustrates that the zeta potential increases as the SNP:ChNC ratio rises. This stems from chitin's highly positive charge at pH 3.0, due to its protonated amino groups. As ChNC proportion increases, its contribution to the overall charge intensifies, raising the zeta potential (Jiménez-Saelices et al., 2020).

Figure 16 – Zeta potential measurements of the aqueous phases (A) and the different SNP:ChNC ratio emulsions (B), for control and HT samples.



Source: Made by the author.

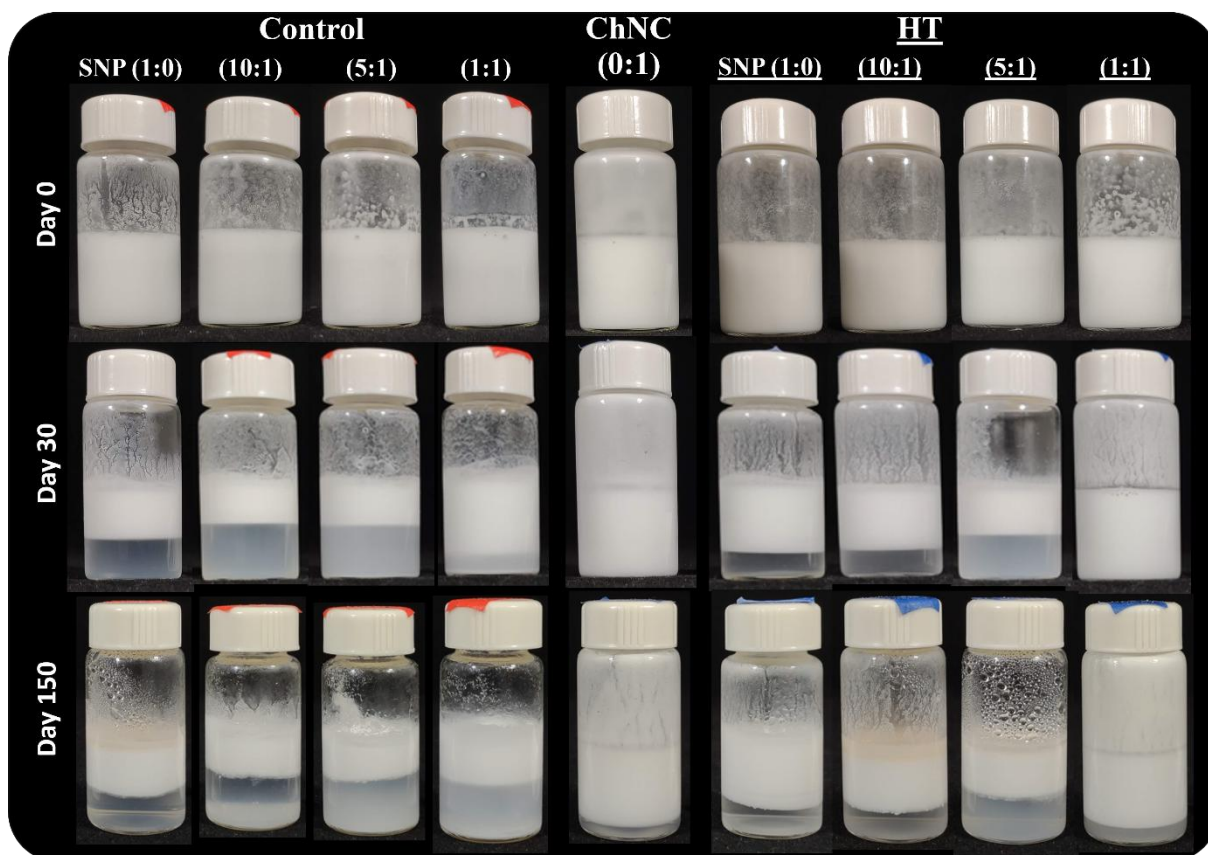
The HT samples exhibited an overall lower zeta potential, a phenomenon due to the swelling of the starch granule and the partial breakage of the double helix starch structure. This process likely resulted in a more flexible and smaller particle with exposed hydroxyl groups that can interact with the positive charge of the chitin, decreasing the zeta potential (Xu et al., 2020). Unlike particles like cellulose nanocrystals, SNP's minimal charge difference compared to ChNC prevents strong binding, allowing them to rearrange freely for optimal positioning within the system, as displayed previously (Figure 14) .

The same kind of behavior is observed in the aqueous phase samples, displaying a higher zeta potential at higher ChNC fractions and a smaller zeta potential for the HT samples. Overall, the emulsions exhibit lower zeta potential than the aqueous phases, likely due to the anionic nature of the oil-water interface. Most food oils (such as soybean, sunflower, and olive oil) exhibit a negatively charged interface, due to the hydroxyl groups of fatty acids projecting into the aqueous phase. In this manner, these negatively charged groups interact electrostatically with the protonated groups of chitin, thereby reducing the zeta potential of the emulsion relative to the aqueous phase (Xiong et al., 2025).

5.3.5 Long-term stability of the Pickering emulsions

The Pickering emulsions (SNP:ChNC ratio of 1:0, 10:1, 5:1, 1:1, 0:1) were observed over 5 months in systems.

Figure 17 – Visual appearance of the control emulsions (non-heat-treated) and the heat-treated (HT) emulsions over time (150 days) with different ratios of SNP:ChNC.



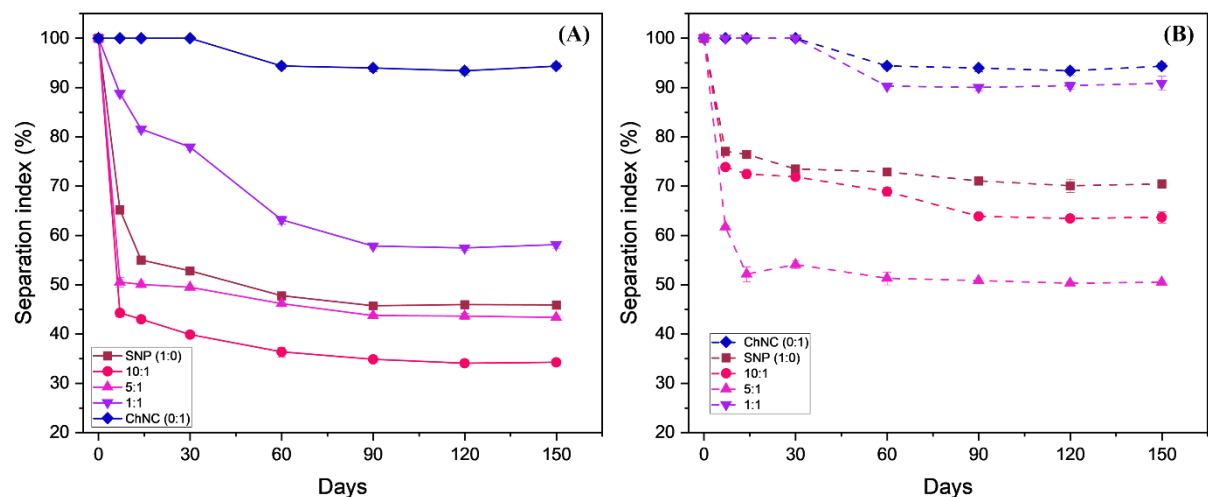
Source: Made by the author.

Pickering emulsions with differences in water/oil density and with a large droplet size are subjected to buoyancy effects, leading to creaming, which is the formation of a cream layer at the top and a serum phase at the bottom of the system (Lu; Xiao; Huang, 2018). The visual appearance of the emulsions (Figure 17) indicates that the efficiency of stabilization can vary significantly depending on the proportion and treatment of the nanoparticles involved. Starch nanoparticles (SNP) without any thermal treatment proved to be unsuitable for emulsion stabilization, as evidenced by significant creaming within 7 days after preparation (25 °C) (Figure 18B). Preheated starch increases the viscosity of the aqueous phase of the emulsion, which favors stabilization by hindering droplet mobility. However, extreme viscosity leads to a dense network, compromising the fluidity of the emulsion and droplet formation during homogenization. The initial addition of ChNC, particularly in samples 10:1 and 5:1, adversely impacted the stabilization process, leading to a higher creaming index compared to the SNP-

only emulsion. However, when the ratio of ChNC was increased (1:1 sample), the two particles showed a synergistic effect, resulting in emulsions with the highest stability.

Interestingly, the 1:1 control emulsion was less stable compared to the ChNC-only emulsion. With the introduction of thermal treatment (HT samples), the samples exhibited a similar reduction in stabilization upon the initial addition of ChNC, mirroring the behavior observed in the control samples (Figure 18A). However, the 1:1 HT sample demonstrated results comparable to those of the ChNC-only emulsion, with creaming only becoming apparent after 1 month at room temperature. This can be attributed to the capacity of the smaller spherical gelatinized starch particles to be tightly packed in the oil-water interface with the chitin (Liu et al., 2018).

Figure 18 – Creaming indexes of the heat treated emulsions control (A) and the HT emulsions (B) with different ratios of SNP:ChNC.



Source: Made by the author.

After 5 months, the difference between the separation indexes of the 1:1 HT and the ChNC-only samples was < 4% (Figure 18B). A better stability to creaming is found for the emulsions prepared by the combination of ChNC and SNP when compared to other starch-based systems, including pea-protein isolate (Y. Liu et al., 2024) and catechin (Park et al., 2024), with the added benefit of the need for no chemical treatment to obtain the SNPs.

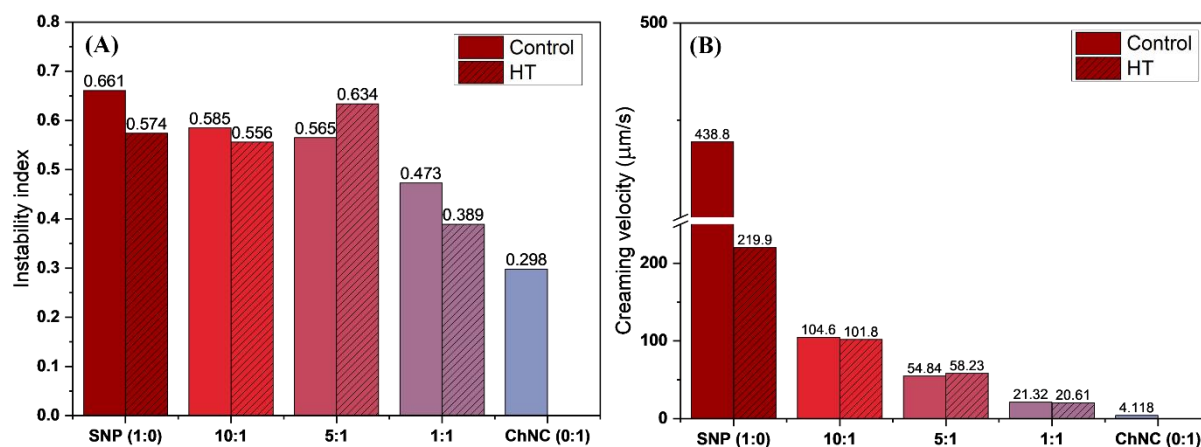
When compared to a chitin-only emulsion, the combination of SNP and ChNC offers several advantages, including reduced costs, improved digestibility, and enhanced potential for drug delivery. ChNC provides positive charges that enhance colloidal suspension stability and

contributes to antibacterial and antifungal properties, which starch alone does not provide (Apriyanto; Compart; Fettke, 2022; Jiménez-Saelices et al., 2020; Lv et al., 2021; Sarkar et al., 2019). Moreover, the two nanoparticles act under different stabilization mechanisms within the emulsion: SNP predominantly localizes at the droplet interfaces, while ChNC enhances inter-droplet stability by forming a network that prevents coalescence, as confirmed by CLSM analyses.

5.3.6 Instability index, creaming velocity, and sedimentation

Centrifugal separation analysis, which the LUMiSizer® uses to record the variation of transmitted light over time and space, provides information on the kinetic separation process of the analyzed samples. Results like the instability index, creaming velocity, and sedimentation velocity can be obtained; these parameters are excellent for comparing the kinetic stability between samples (Zielińska et al., 2018).

Figure 19 – Instability index (A) and creaming velocity (B) obtained via accelerated stability analysis for the different SNP:ChNC ratio emulsions, both control and HT at 21 °C.

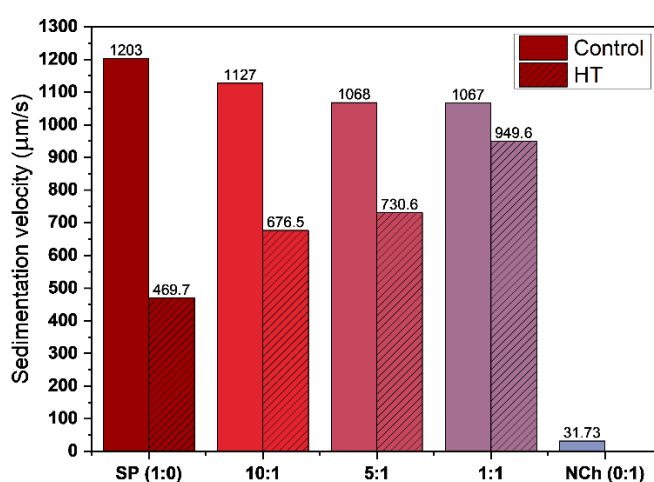


Source: Made by the author.

The instability index of the ChNC-only emulsion was the lowest one compared to all other samples (Figure 19A). The addition of chitin initially has an adverse effect on the instability index of the HT emulsions which corroborate with the visual results of stability over time (Figure 17), but when the concentration of SNP and ChNC were the same, sample 1:1, the instability index was lower for both control and HT samples. Between the SNP plus ChNC samples the 1:1 sample exhibited the best result.

When looking at the creaming velocity (Figure 19B) of all the samples a more revealing result can be attained, there was an obvious decrease in the velocity with the addition of the chitin, even though the initial concentrations of chitin had an adverse effect on the stability as seen in Figure 17 and Figure 19A, at the very beginning of the destabilization process the chitin helps the system, evidenced by the low creaming velocity. Once again, the best results between the SNP plus ChNC samples were displayed by the 1:1 sample.

Figure 20 – Sedimentation velocity obtained via accelerated stability analysis for the different SNP:ChNC ratio aqueous phase, both control and HT.



Source: Made by the author.

The sedimentation velocity of the SNP and chitin particles in the HT samples was lower in the aqueous phase (Figure 20) than that of the control samples, suggesting that these suspensions are more stable than the control ones. The HT samples show an increase in sedimentation velocity with the addition of chitin, whereas the control samples do not show as much variation in sedimentation velocity with the increase of chitin fraction. This may be because the more flexible and softer gelatinized starch particles interact better with the ChNC to form denser particles that sediment more quickly than when the two components are mixed but not pre heated (Liu et al., 2018; Xu et al., 2020).

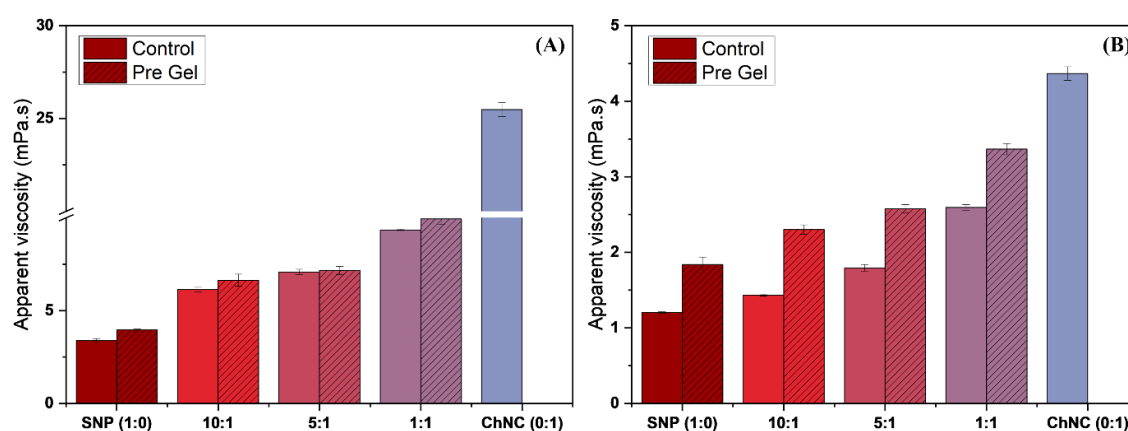
5.3.7 Viscosity assays

This increasing viscosity of the aqueous phase with the addition of chitin shows the same behavior as the sedimentation velocities of these samples (Figure 20) showing the influence of the viscosity in the sedimentation process.

The higher viscosity observed in the 1:1 HT and ChNC aqueous phase suggests that the increased viscosity of the aqueous phase serves as a key stabilizing mechanism in the emulsions. This elevated viscosity plays a crucial role in maintaining inter-droplet stability. Additionally, the viscosity enhancement provided by chitin nanocrystals (ChNC) is complemented by conformational changes in amylose and amylopectin structures within the starch, particularly in the heat-treated (HT) samples. These structural transformations further contribute to the overall increase in viscosity, reinforcing emulsion stability (Hussain Badar et al., 2024; Velandia et al., 2021).

The apparent viscosity (Figure 21A) of the HT emulsion samples were, in most cases, slightly higher than their control counterparts, which was expected because of the heat treatment that causes the full gelatinization of all the starch granules, even though the difference was not as big as expected. However, the same comparison in the aqueous phase (Figure 21B) posed a more noticeable difference, that higher viscosity, in the HT aqueous phases, comes from the interaction of the HT SNP, that by itself is a great thickening agent, and the ChNC (Xu et al., 2020).

Figure 21 – Apparent viscosity (100s⁻¹) for the different SNP:ChNC ratio emulsions (A) and their respective aqueous phase (B), both control and HT samples.



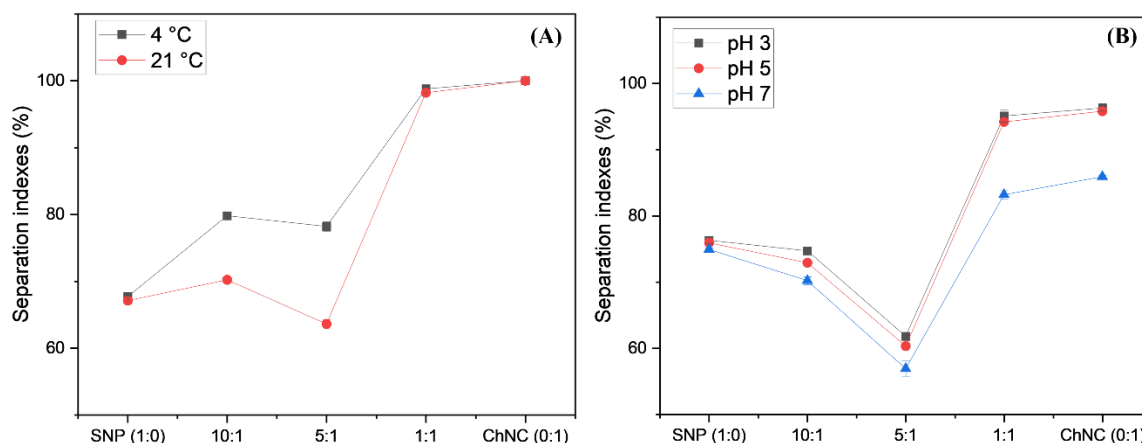
Source: Made by the author.

The emulsion samples showed an overall higher viscosity than the aqueous phase samples due to being a more complex and structured system because of the presence of oil droplets. The ChNC emulsion displayed the highest viscosity between all the samples, this is due to the gel forming effect that ChNC has when used in the stabilization of Pickering emulsions specially in lower pH values (<6,8) (Jiménez-Saelices et al., 2020; Sara et al., 2019). The higher viscosity values (1:1 HT and ChNC) can be directly associated with the bridge-forming behavior of the ChNC discussed in the previous topic (5.3.2). The values of viscosity obtained for the emulsions studied were within the range reported in the literature for starch stabilized Pickering emulsions. The low viscosity of the samples is of good interest for functional beverages applications (Cai; Zhang; Xie, 2024).

5.3.8 pH and temperature stability

Figure 22 shows the creaming indexes for the studied HT emulsions under different temperature and pH storages at the day of preparation and after 7 days of storage.

Figure 22 – Separation indexes for the studied HT Pickering emulsions under different temperatures (A) and pH (B) conditions, after 7 days of storage.



Source: Made by the author.

Figure 22A demonstrates that the stability of the emulsions improves when stored at cooler temperatures. This suggests that a potential final product utilizing this emulsion system could have an extended shelf life if kept in a cool environment, such as a refrigerator. Enhanced stability is likely due to the thickening of liquids and colloidal systems, such as Pickering emulsions, at lower temperatures, which helps to inhibit coalescence (Ding et al., 2019).

The emulsions also showed lower stabilities at higher pHs, for those with higher ChNC content this event is even more expressive, due to the better colloidal stability of chitin on acidic pHs, which would disrupt the effect of the ChNC on the bulk of the aqueous phase making it easier for coalescence to happen which leads to emulsion destabilization. But the emulsions still show satisfactory stability on the studied pHs which are the most common pH range for food products, indicating these emulsions would be stable to be used as ingredients in food products in this pH range (Zhong et al., 2024).

5.4 Conclusions

In conclusion, the synergistic combination of SNP and ChNC has shown significant potential as an alternative particle systems for stabilizing oil-in-water Pickering emulsions relevant to food formulations. The emulsions also offer functional promise as far as antimicrobial activity (ChNC), digestibility and cost-effectiveness (SNP).

Our findings reveal that SNP and ChNC contribute to emulsion stability through distinct mechanisms. The introduction of a simple heat treatment step in the aqueous phase before emulsification proved to be a highly effective strategy, drastically enhancing emulsion stability. Among the tested formulations, the 1:1 SNP:ChNC ratio consistently outperformed other combinations, demonstrating superior stability across multiple parameters. The emulsions remained stable under varying temperatures and pH conditions during storage, reinforcing their suitability for food applications.

The SNP-ChNC system is more cost-effective compared to ChNC-only emulsions and offers a sustainable alternative to chemically modified SNP. The differing digestibility and bioavailability of SNP and ChNC provide further opportunities for tailoring the system's nutritional properties. Overall, this research underscores the potential of SNP-ChNC combinations in developing stable, customizable Pickering emulsions for food formulations.

5 CONCLUSÕES GERAIS

Em conclusão, o processo de moagem de bolas, especialmente com uma duração de 10 horas e uma razão de massa de 1:20 de amido para esferas, promove uma transformação significativa nos grânulos de amido, resultando em uma intensificação da reatividade e redução da temperatura de gelatinização. O amido assim obtido por moagem demonstra ser um agente espessante apropriado, notadamente em aplicações termicamente sensíveis, como na indústria farmacêutica e em produtos alimentícios específicos. Este estudo revela, sobretudo, a alta influência de um procedimento aparentemente elementar, como a moagem, na temperatura de gelatinização do amido e em suas propriedades reológicas. No contexto da sinergia entre nanopartículas de amido (SNP) e nanocristais de quitina (ChNC), determinamos que é uma promissora combinação de polímeros alternativa para a estabilização de emulsões Pickering óleo-em-água, especialmente relevante na indústria alimentícia. Ao unir a carga positiva e as propriedades antimicrobianas da quitina com a digestibilidade e economia do amido, essa abordagem inovadora se mostra multifacetada. A introdução de uma etapa de pré-gelatinização antes da emulsificação se mostrou como uma estratégia simples, mas altamente eficaz, contribuindo para o melhoramento da estabilidade das emulsões Pickering. Entre as emulsões investigadas, destaca-se consistentemente a amostra com proporção 1:1 em relação às demais emulsões de SNP e ChNC, evidenciando sua superioridade em diversos parâmetros e ressaltando o potencial de formulações personalizadas para o desenvolvimento estável de emulsões Pickering.

REFERÊNCIAS

ABEGUNDE, Oluwaseyi Kemi et al. Physicochemical characterization of sweet potato starches popularly used in Chinese starch industry. **Food Hydrocolloids**, v. 33, n. 2, p. 169–177, 2013.

AGAMA-ACEVEDO, Edith; BELLO-PEREZ, Luis A. Starch as an emulsions stability: the case of octenyl succinic anhydride (OSA) starch. **Current Opinion in Food Science**, v. 13, n. 3 p. 78–83, 2017.

AHMAD, Mudasir et al. Influence of ball milling on the production of starch nanoparticles and its effect on structural, thermal and functional properties. **International Journal of Biological Macromolecules**, v. 151, n. 3, p. 85–91, 2020.

APOSTOLIDIS, Eftychios. Production of nanoparticles from resistant starch via a simple three-step physical treatment. **Food Hydrocolloids**, v. 137, n. 3, p. 88–92, 2023.

APRIYANTO, Ardha; COMPART, Julia; FETTKE, Joerg. A review of starch, a unique biopolymer – Structure, metabolism and in planta modifications. **Plant Science**, v. 318, p. 111–223, 2022.

ASABUWA NGWABEBHOH, Fahanwi; ILKAR ERDAGI, Sevinc; YILDIZ, Ufuk. Pickering emulsions stabilized nanocellulosic-based nanoparticles for coumarin and curcumin nanoencapsulations: In vitro release, anticancer and antimicrobial activities. **Carbohydrate Polymers**, v. 201, p. 317–328, 2018.

AZFARALARIFF, Ahmad et al. Food-grade particle stabilized Pickering emulsion using modified sago (Metroxylon sagu) starch nanocrystal. **Journal of Food Engineering**, v. 280, 2020.

BAI, Long et al. Oil-in-water Pickering emulsions via microfluidization with cellulose nanocrystals: 1. Formation and stability. **Food Hydrocolloids**, v. 96, p. 699–708, 2019.

BAI, Long et al. Recent advances in food emulsions and engineering food stuffs using plant-based nanocelluloses. **Annual Review of Food Science and Technology**. 2021, v. 12, 2021.

BANGAR, Sneha Punia et al. Ball-milling: A sustainable and green approach for starch modification. **International Journal of Biological Macromolecules**. v. 15, p. 90-100, 2023.

BARROS, Matheus de Oliveira et al. Effect of ball-milling on starch crystalline structure, gelatinization temperature, and rheological properties: towards enhanced utilization in thermosensitive systems. **Foods**, v. 12, n. 15, 2023.

BEN CHEIKH, Fatma et al. Chitin nanocrystals as Pickering stabilizer for O/W emulsions: Effect of the oil chemical structure on the emulsion properties. **Colloids and Surfaces B: Biointerfaces**, v. 200, p. 511-604, 2021.

BERTON-CARABIN, Claire C.; SCHROËN, Karin. Pickering emulsions for food applications: Background, trends, and challenges. **Annual Review of Food Science and Technology Annual Reviews Inc**. v. 20, n. 3, p. 115 – 125, 2015.

CABRITA, Marta et al. Development of innovative clean label emulsions stabilized by vegetable proteins. **International Journal of Food Science and Technology**, v. 58, p. 406–422, 2023.

CAI, Jie; ZHANG, Die; XIE, Fang. The role of alginate in starch nanocrystals-stabilized Pickering emulsions: From physical stability and microstructure to rheology behavior. **Food Chemistry**, v. 431, p. 13-37, 2024.

CHAKRABORTY, Ishita et al. An Insight into the Gelatinization Properties Influencing the Modified Starches Used in Food Industry: A review. **Food and Bioprocess Technology**, v. 235, n. 3, p 20-35, 2022.

CHEN, Ruiyun et al. The interaction of pectin with wheat starch and its influence on gelatinization and rheology. **Food Hydrocolloids**, v. 136, p. 77-88, 2023.

CHEVALIER, Yves; BOLZINGER, Marie Alexandrine. Emulsions stabilized with solid nanoparticles: Pickering emulsions. **Colloids and Surfaces A: Physicochemical and Engineering Aspects**, v. 439, p. 23–34, 2013.

CHRASTIL, Joseph. Improved colorimetric determination of amylose in starch flours. **Carbohydrate Research**, p. 154–158, 1987.

CUI, Congli et al. Bioactive and intelligent starch-based films: A review. **Trends in Food Science and Technology**, v. 116, p. 854–869, 2021a.

CUI, Fengzhan et al. Polysaccharide-based Pickering emulsions: Formation, stabilization and applications. **Food Hydrocolloids**, v. 119, 2021b.

DE DIOS-AVILA, Ndahita et al. Physicochemical, Structural, Thermal, and Rheological Properties of Mango Seed Starch from Five Cultivars. **Polysaccharides**, v. 5, n. 4, p. 872–891, 2024.

DESAM, Gnana Prasuna et al. Characterization of storage modulus of starch suspensions during the initial stages of pasting using Stokesian dynamics simulations. **Food Hydrocolloids**, v. 121, p. 268–273, 2021.

DING, Mengzhen et al. Effect of preparation factors and storage temperature on fish oil-loaded crosslinked gelatin nanoparticle pickering emulsions in liquid forms. **Food Hydrocolloids**, v. 95, p. 326–335, 2019.

DOKIĆ, Ljubica; KRSTONOŠIĆ, Veljko; NIKOLIĆ, Ivana. Physicochemical characteristics and stability of oil-in-water emulsions stabilized by OSA starch. **Food Hydrocolloids**, v. 29, n. 1, p. 185–192, 2012.

EHSANI, Ali et al. Bioemulsifiers derived from microorganisms: applications in the drug and food industry. **Advanced Pharmaceutical Bulletin**, v. 8, n. 2, p. 191–199, 2018.

FACCHINE, Emily G. et al. Associative structures formed from cellulose nanofibrils and nanochitins are pH-responsive and exhibit tunable rheology. **Journal of Colloid and Interface Science**, v. 588, p. 232–241, 2021.

FRANZOL, Angélica; REZENDE, Mirabel Cerqueira. Estabilidade de emulsões: um estudo de caso envolvendo emulsionantes aniônico, catiônico e não-iônico. **Polimeros**, v. 25, p. 1–9, 2015.

FU, Zong Qiang et al. Effects of partial gelatinization on structure and thermal properties of corn starch after spray drying. **Carbohydrate Polymers**, v. 88, n. 4, p. 1319–1325, 2012.

GOIANA, Mayara Lima et al. Corn starch based films treated by dielectric barrier discharge plasma. **International Journal of Biological Macromolecules**, v. 183, p. 2009–2016, 2021.

GUIDA, Carolina; AGUIAR, Ana Carolina; CUNHA, Rosiane Lopes. Green techniques for starch modification to stabilize Pickering emulsions: a current review and future perspectives. **Current Opinion in Food Science**, v. 38, p. 52–61, 2021.

GUO, Shasha et al. Heteroaggregation effects on Pickering stabilization using oppositely charged cellulose nanocrystal and nanochitin. **Carbohydrate Polymers**, v. 299, p. 100-125, 2023.

HADI, N. Abdul et al. Characterization and stability of short-chain fatty acids modified starch Pickering emulsions. **Carbohydrate Polymers**, v. 29, p. 90-115, 2020.

HAN, Fei et al. Synthesis, optimization and characterization of acetylated corn starch with the high degree of substitution. **International Journal of Biological Macromolecules**, v. 59, p. 372–376, 2013.

HAN, Ni et al. Effect of ball milling treatment on the structural, physicochemical and digestive properties of wheat starch, A- and B-type starch granules. **Journal of Cereal Science**, v. 104, p. 24-39, 2022.

HU, Jianbo et al. Dissolution of starch in urea/NaOH aqueous solutions. **Journal of Applied Polymer Science**, v. 133, n. 19, 2016.

HUANG, Zu Qiang et al. Ball-milling treatment effect on physicochemical properties and features for cassava and maize starches. **Comptes Rendus Chimie**, v. 11, n. 1–2, p. 73–79, 2008.

HUSSAIN BADAR, Iftikhar et al. Influence of varying oil phase volume fractions on the characteristics of flaxseed-derived diglyceride-based Pickering emulsions stabilized by modified soy protein isolate. **Food Research International**, v. 175, p. 963–9969, 2024.

Ji, Chuye; WANG, Yixiang. Lignin-containing cellulose nanocrystals from maple leaves: A natural Pickering emulsion stabilizer for food preservation. **Food Chemistry**, v. 463, 15 2025.

JIMÉNEZ-SAELICES, Clara et al. Chitin Pickering Emulsion for Oil Inclusion in Composite Films. **Carbohydrate Polymers**, v. 29, p. 100–111, 2020.

JONES, Mitchell et al. Crab vs. Mushroom: a review of crustacean and fungal chitin in wound treatment. **Marine Drugs**, v. 18, n. 1, p. 64, 2020.

KALASHNIKOVA, Irina et al. Cellulosic nanorods of various aspect ratios for oil in water Pickering emulsions. **Soft Matter**, v. 9, n. 3, p. 952–959, 2013.

KERAMAT, Malihe; KHEYNOOR, Najme; GOLMAKANI, Mohammad-Taghi. Oxidative stability of Pickering emulsions. **Food Chemistry: X**, v.8, n.1, p. 22–35, 2022.

KO, Eun Byul; KIM, Jong Yea. Application of starch nanoparticles as a stabilizer for Pickering emulsions: Effect of environmental factors and approach for enhancing its storage stability. **Food Hydrocolloids**, v. 120, 2021.

LARBI, Fatma et al. Comparison of nanocrystals and nanofibers produced from shrimp shell α -chitin: From energy production to material cytotoxicity and Pickering emulsion properties. **Carbohydrate Polymers**, v. 8, p. 15–26, 2018.

LE CORRE, Déborah; BRAS, Julien; DUFRESNE, Alain. Starch nanoparticles: A review. **Biomacromolecules**, v. 12, n. 2, p. 30-46, 2010.

LEAL-LAZARENO, Cinthya G. et al. Structural, molecular, and physicochemical properties of starch in high-amylose durum wheat lines. **Food Hydrocolloids**, v. 160, p. 77-91, 2025.

LEE, Matthew N.; CHAN, Hubert K.; MOHRAZ, Ali. Characteristics of Pickering emulsion gels formed by droplet bridging. **Langmuir**, v. 28, n. 6, p. 3085–3091, 2012.

LI, Enpeng; DHITAL, Sushil; HASJIM, Jovin. Effects of grain milling on starch structures and flour/starch properties. **Starch/Staerke**, v. 15, n. 5, p. 125-145, 2014.

LI, Jiali et al. Preparation of oxidized corn starch with high degree of oxidation by fenton-like oxidation assisted with ball milling. **Materials Today Communications**, v. 22, n. 3, 2020.

LIMPONGSA, Ekapol; SOE, May Thu; JAIPAKDEE, Napaphak. Modification of release and penetration behavior of water-soluble active ingredient from ball-milled glutinous starch matrix via carboxymethylcellulose blending. **International Journal of Biological Macromolecules**, v. 193, p. 2271–2280, 2021.

LIU, Cancan et al. Pickering emulsions stabilized by compound modified areca taro (*Colocasia esculenta* (L.) Schott) starch with ball-milling and OSA. **Colloids and Surfaces A: Physicochemical and Engineering Aspects**, v. 556, p. 185–194, 2018a.

LIU, Chong; HONG, Jing; ZHENG, Xueling. Effect of heat-moisture treatment on morphological, structural and functional characteristics of ball-milled wheat starches. **Starch/Staerke**, v. 69, n. 5–6, 2017.

LIU, Dagang et al. Transitional properties of starch colloid with particle size reduction from micro- to nanometer. **Journal of Colloid and Interface Science**, v. 339, n. 1, p. 117–124, 2009.

LIU, Wei et al. Stabilizing Oil-in-Water Emulsion with Amorphous and Granular Octenyl Succinic Anhydride Modified Starches. **Journal of Agricultural and Food Chemistry**, v. 66, n. 35, p. 9301–9308, 2018b.

LIU, Wei et al. Interfacial Activity and Self-Assembly Behavior of Dissolved and Granular Octenyl Succinate Anhydride Starches. **Langmuir**, v. 35, n. 13, p. 4702–4709, 2019.

LIU, Xingxun et al. Thermal degradation and stability of starch under different processing conditions. **Starch/Stärke**, v. 65, n. 1–2, p. 48–60, 2013.

LIU, Xin-Yue et al. Modulation of pea protein isolate nanoparticles by interaction with OSA-corn starch: Enhancing the stability of the constructed Pickering emulsions. **Food Chemistry**, v. 437, p. 13-66, 2024a.

LIU, Zhanna et al. Preparation and characterization of bacterial cellulose by kombucha using corncob. **Cellulose**, v. 12, n. 2, p. 95-112, 2024b.

LOPES, Isadora S. et al. Effect of chitosan size on destabilization of oil/water emulsions stabilized by whey protein. **Colloids and Surfaces A: Physicochemical and Engineering Aspects**, v. 574, p. 207–214, 2019.

LU, Hao; TIAN, Yaoqi. Nanostarch: Preparation, Modification, and Application in Pickering Emulsions. **Journal of Agricultural and Food Chemistry**, v. 10, n. 3, p. 115-130, 2021a.

LU, Hao; TIAN, Yaoqi. Nanostarch: Preparation, Modification, and Application in Pickering Emulsions. **Journal of Agricultural and Food Chemistry**, v. 69, n. 25, p. 6929–6942, 2021b.

LU, Xuanxuan; XIAO, Jie; HUANG, Qingrong. Pickering emulsions stabilized by media-milled starch particles. **Food Research International**, v. 105, p. 140–149, 2018.

LV, Shanshan et al. Development of food-grade Pickering emulsions stabilized by a mixture of cellulose nanofibrils and nanochitin. **Food Hydrocolloids**, v. 113, p. 85-96, 2021.

MA, Hao et al. Research progress on properties of pre-gelatinized starch and its application in wheat flour products. **Grain and Oil Science and Technology**, v. 11, n.3, p.115-125, 2022.

MA, Shuping; ZHU, Peilei; WANG, Mingchun. Effects of konjac glucomannan on pasting and rheological properties of corn starch. **Food Hydrocolloids**, v. 89, p. 234–240, 2019.

MA, Yaomei et al. Insoluble dietary fiber stabilized Pickering emulsions as novel food ingredients: Preparation, potential applications and future perspectives. **Food Chemistry**, v. 15, n. 2, p. 25-45, 2025.

MANDALA, I. G.; BAYAS, E. Xanthan effect on swelling, solubility and viscosity of wheat starch dispersions. **Food Hydrocolloids**, v. 18, n. 2, p. 191–201, 2004.

MARENCO-OROZCO, Gerald A.; ROSA, Morsyleide F.; FERNANDES, Fabiano A. N. Effects of multiple-step cold plasma processing on banana (*Musa sapientum*) starch-based films. **Packaging Technology and Science**, v. 35, n. 8, p. 589–601, 2022.

MARTA, Herlina et al. Starch Nanoparticles: Preparation, Properties and Applications. **Polymers**, v. 15, n. 5, 2023.

MARTO, Joana et al. Starch-based pickering emulsions as platforms for topical antibiotic delivery: In vitro and in vivo studies. **Polymers**, v. 11, n. 1, 2019.

MCCLEMENTS, David Julian. Food Emulsions: Principles, Practices, and Techniques. 3. ed. Massachusetts : CRC Press. 2016.

MCCLEMENTS, David Julian; BAI, Long; CHUNG, Cheryl. Recent Advances in the Utilization of Natural Emulsifiers to Form and Stabilize Emulsions. **Annual Review of Food Science and Technology**, v. 8, p. 205–236, 2017.

MCCLEMENTS, David Julian; JAFARI, Seid Mahdi. Historical perspective Improving emulsion formation, stability and performance using mixed emulsifiers: A review. **PubMed**, v.15, n. 1, p. 1- 15, 2017.

MCCLEMENTS, David Julian; LU, Jiakai; GROSSMANN, Lutz. Proposed Methods for Testing and Comparing the Emulsifying Properties of Proteins from Animal, Plant, and Alternative Sources. **Colloids and Interfaces**, v. 12, n. 2, p. 25-45, 2022.

MOHAMMAD AMINI, Asad; RAZAVI, Seyed Mohammad Ali. A fast and efficient approach to prepare starch nanocrystals from normal corn starch. **Food Hydrocolloids**, v. 57, p. 132–138, 2016.

MUÑOZ-NÚÑEZ, Carolina; FERNÁNDEZ-GARCÍA, Marta; MUÑOZ-BONILLA, Alexandra. Chitin Nanocrystals: Environmentally Friendly Materials for the Development of Bioactive Films. **Coatings**, v. 12, n. 2, p. 110-115, 2022.

MWANGI, William Wachira et al. Food-grade Pickering emulsions for encapsulation and delivery of bioactives. **Trends in Food Science and Technology**, v. 100, p. 320–332, 2020.

NARCISO, Joan Oñate et al. Pickering Emulsions as Catalytic Systems in Food Applications. **Food Science and Technology**, v. 5, p. 35, 2025.

NARPINDER, Singh et al. Morphological, thermal and rheological properties of starches from different botanical sources. **Food Chemistry**, v. 81, p. 1–31, 2003.

OLIVEIRA, Ana Vitória et al. Nanocomposite Films from Mango Kernel or Corn Starch with Starch Nanocrystals. **Starch/Staerke**, v. 70, n. 11–12, 2018a.

OLIVEIRA, C. S. et al. Effect of ball milling on thermal, morphological and structural properties of starches from zingiber officinale and dioscorea sp. **Carpathian Journal of Food Science and Technology**, v. 10, n. 4, p. 90–103, 2018b.

PAREDES-TOLEDO, Javier et al. Pickering Double Emulsions Stabilized with Chitin Nanocrystals and Myristic Acid-Functionalized Silica Nanoparticles for Curcumin and Chlorogenic Acid Co-Delivery. **Pharmaceutics**, v. 17, n. 4, p. 521, 2025.

PARK, Jae Young et al. Preparation of catechin-starch nanoparticles composites and its application as a Pickering emulsion stabilizer. **Carbohydrate Polymers**, v. 15, n. 2, p. 225-235, 2024.

PARK, Shinjae; KIM, Yong Ro. Clean label starch: production, physicochemical characteristics, and industrial applications. **Food Science and Biotechnology**, v. 30, n. 1, 2021.

PÉREZ, Serge; BERTOFT, Eric. The molecular structures of starch components and their contribution to the architecture of starch granules: A comprehensive review. **Starch/Staerke**, v. 62, n. 8, p. 389–420, 2010.

PICKERING, Spencer Umfreville. CXCVI. - Emulsions. **Journal of the Chemical Society**, v. 34, n. 2, p. 25-35, 1907.

POZO, Claudio et al. Study of the structural order of native starch granules using combined FTIR and XRD analysis. **Journal of Polymer Research**, v. 25, n. 12, 2018.

RODRIGUEZ-GARCIA, Mario Enrique et al. Crystalline structures of the main components of starch. **Current Opinion in Food Science**, v. 37, p. 107–111, 2021.

SARA, Merin et al. Starch, Chitin, Chitosan Based Composites and Nanocomposites. **Springer**, v. 1, n. 2, p. 24-45, 2019.

SARKAR, Anwesha et al. Colloidal aspects of digestion of Pickering emulsions: Experiments and theoretical models of lipid digestion kinetics. **Advances in Colloid and Interface Science**, v. 12, n. 2, p. 13-45, 2019.

SHI, Jialiang; SWEEDMAN, Michael C.; SHI, Yong Cheng. Structure, birefringence and digestibility of spherulites produced from debranched waxy maize starch. **International Journal of Biological Macromolecules**, v. 183, p. 1486–1494, 2021.

SIKORA, Marek et al. Thixotropic properties of normal potato starch depending on the degree of the granules pasting. **Carbohydrate Polymers**, v. 121, p. 254–264, 2015.

SILVA, Ana Priscila M. et al. Mango kernel starch films as affected by starch nanocrystals and cellulose nanocrystals. **Carbohydrate Polymers**, v. 211, p. 209–216, 2019.

SINGH, Jaspreet; KAUR, Lovedeep; MCCARTHY, O. J. Factors influencing the physico-chemical, morphological, thermal and rheological properties of some chemically modified starches for food applications-A review. **Food Hydrocolloids**, v. 2, n. 2, p. 25-45, 2007.

SU, Xiaoya et al. Control of the colloidal and adsorption behaviors of chitin nanocrystals and an oppositely charged surfactant at solid, liquid, and gas interfaces. **Langmuir**, v. 10, n. 2, p. 11-35, 2024.

TAMAKI, Shinji et al. Structural Change of Maize Starch Granules by Ball-mill Treatment. **Starch/Stärke**, v. 8, p. 342–348, 1998.

THRAEIB, Jaffar Z. et al. Production and characterization of a bioemulsifier derived from microorganisms with potential application in the food industry. **Life**, v. 12, p. 1-25, 2022.

TORRES, Fernando G.; DE-LA-TORRE, Gabriel E. Synthesis, characteristics, and applications of modified starch nanoparticles: A review. **International Journal of Biological Macromolecules**, v. 10, p. 45-56, 2022

UNITED NATIONS. Transforming our world: the 2030 Agenda for Sustainable Development. Disponível em: <<https://sdgs.un.org/2030agenda>>. Acesso em: 13 maio. 2025.

VAN SOEST, Jeroen JG et al. Short-range structure in (partially) crystalline potato starch determined with attenuated total reflectance Fourier-transform IR spectroscopy. **Carbohydrate Research**, v. 279, p. 201–214, 1995.

VELANDIA, Santiago F. et al. Evaluation of the repartition of the particles in Pickering emulsions in relation with their rheological properties. **Journal of Colloid and Interface Science**, v. 589, p. 286–297, 2021.

WANG, Ke et al. The degree of substitution of OSA-modified starch affects the retention and release of encapsulated mint flavour. **Carbohydrate Polymers**, v. 294, p. 65-91, 2022.

WATERSCHOOT, Jasmien; GOMAND, Sara V.; DELCOUR, Jan A. Impact of swelling power and granule size on pasting of blends of potato, waxy rice and maize starches. **Food Hydrocolloids**, v. 52, p. 69–77, 2016.

WINUPRASITH, Thunnalin et al. Encapsulation of vitamin D3 in pickering emulsions stabilized by nanofibrillated mangosteen cellulose: Impact on vitro digestion and bioaccessibility. **Food Hydrocolloids**, v. 83, p. 153–164, 2018.

XIONG, Zhouyi et al. Chitin nanofiber-stabilized pickering emulsion interacting with egg white protein: Structural features, interfacial properties, and stability. **Food Hydrocolloids**, v. 161, 2025.

XU, Tian et al. Characteristics of starch-based Pickering emulsions from the interface perspective. **Trends in Food Science & Technology**, v. 105, p. 334–346, 2020.

XU, Tian et al. Formation, stability and the application of Pickering emulsions stabilized with OSA starch/chitosan complexes. **Carbohydrate Polymers**, v. 299, p. 225-245, 2023.

YANG, Sha et al. Structural, gelatinization, and rheological properties of heat-moisture treated potato starch with added salt and its application in potato starch noodles. **Food Hydrocolloids**, v. 131, 2022.

YANG, Zhen et al. Pickering emulsions stabilized by soybean protein–based nanoparticles: A review of formulation, characterization, and food-grade applications. **Comprehensive Reviews in Food Science and Food Safety**, v. 24, n. 2, 2025.

YE, Qianyu; GEORGES, Nicolas; SELOMULYA, Cordelia. Microencapsulation of active ingredients in functional foods: From research stage to commercial food products. **Trends in Food Science and Technology**, v. 78, p. 167–179, 2018.

ZHANG, Kexin et al. Low-pressure plasma modification of the rheological properties of tapioca starch. **Food Hydrocolloids**, v. 125, 2022.

ZHANG, Luyao et al. Effects of amylose and amylopectin fine structure on the thermal, mechanical and hydrophobic properties of starch films. **International Journal of Biological Macromolecules**, v. 282, 2024.

ZHONG, Weiquan et al. pH-responsive Pickering emulsion containing citrus essential oil stabilized by zwitterionically charged chitin nanofibers: Physicochemical properties and antimicrobial activity. **Food Chemistry**, v. 433, 2024.

ZHOU, Hualu et al. Modulation of Physicochemical Characteristics of Pickering Emulsions: Utilization of Nanocellulose- And Nanochitin-Coated Lipid Droplet Blends. **Journal of Agricultural and Food Chemistry**, v. 68, n. 2, p. 603–611, 2020a.

ZHOU, Hualu et al. Nanochitin-stabilized pickering emulsions: Influence of nanochitin on lipid digestibility and vitamin bioaccessibility. **Food Hydrocolloids**, v. 106, 2020b.

ZHOU, Hualu et al. Chitin nanocrystals reduce lipid digestion and β -carotene bioaccessibility: An in-vitro INFOGEST gastrointestinal study. **Food Hydrocolloids**, v. 113, 2021.

ZHU, Fan. Starch based Pickering emulsions: Fabrication, properties, and applications. **Trends in Food Science and Technology**, v. 85, n. 1, p. 129–137, 2019.

ZHU, Mengqi et al. Recent development in food emulsion stabilized by plant-based cellulose nanoparticles. **Current Opinion in Colloid and Interface Science**, v. 15, p. 235-251, 2021.

ZIA-UD-DIN; XIONG, Hanguo; FEI, Peng. Physical and chemical modification of starches: A review. **Critical Reviews in Food Science and Nutrition**, v. 57, n. 12, p. 2691–2705, 2017.

ZIELIŃSKA, Aleksandra et al. Anti-inflammatory and anti-cancer activity of citral: Optimization of citral-loaded solid lipid nanoparticles (SLN) using experimental factorial design and LUMiSizer®. **PubMed**, v. 10, n. 2, p. 35-48, 2018.